QUICS: Quantifying Uncertainty in Integrated Catchment Studies

D3.2 Enhanced algorithms to quantify uncertainty in radar rainfall measurement

Lead: University of Bristol

Revision: 22 Nov 2017

Report Details

Title: Enhanced algorithms to quantify uncertainty in radar rainfall measurement

Deliverable Number (If applicable): 3.2

Author(s): Francesca Cecinati (FC), Miguel A. Rico-Ramirez (MRR)

Document History

Version	Date	Status	Submitted by	Checked by	Comment
1	17/10/2017	Outline	Francesca Cecinati	Miguel A. Rico-Ramirez	
2	31/10/2017	Final Draft	Francesca Cecinati	Miguel A. Rico-Ramirez	Minor changes
3	22/11/2017	Final Version	Miguel A. Rico-Ramirez and Francesca Cecinati	Gerard Heuvelink	

Acronyms and Abbreviations

AR(1)	Auto-Regressive Model Order 1
AR(2)	Auto-Regressive Model Order 2
BK	Block Kriging
CDF	Cumulative Distribution Function
CEH	Centre for Environment and Hydrology
CK	Co-Kriging
CM	Conditional Merging
CSO	Combined Sewer Overflow
DEM	Digital Elevation Model
DSD	Drop Size Distribution
DWD	Deutscher Wetterdienst (German Meteorological Office)

EA	Environment Agency
EU	European Union
FFT	Fast Fourier Transform
ICM	Integrated Catchment Model
KED	Kriging with External Drift
KED-NSV	Kriging with External Drift and Non-Stationary Variance
KEDUD	Kriging with External Drift for Uncertain Data
KNMI	Koninklijk Nederlands Meteorologisch Instituut (Royal Netherlands Meteorological Institute)
KUD	Kriging for Uncertain Data
NWP	Numerical Weather Prediction
OK	Ordinary Kriging
OK1	Ordinary Kriging with 1 rain gauge
OKUD	Ordinary Kriging for Uncertain Data
OKUD1	Ordinary Kriging for Uncertain Data with 1 rain gauge
PDF	Probability Distribution Function
QPE	Quantitative Precipitation Estimation
QUICS	Quantifying Uncertainty in Integrated Catchment Studies
REAL	radar ensemble generator using LU decomposition
REML	Restricted Maximum Likelihood
SCE-UA	Shuffled Complex Evolution method - University of Arizona
TBR	Tipping Bucket Rain gauge
VRP	Vertical Reflectivity Profile
WFD	Water Framework Directive
WWTP	Waste Water Treatment Plant

Executive Summary

Weather radars have significantly improved our ability to measure and understand rainfall processes, thanks to the ability to perform spatial measurements on vast areas at high spatial and temporal resolutions. However, the application of radar rainfall data in hydrological and in water quality models is limited by the lower accuracy that radar data can reach, compared to point rain gauge rainfall measurements. On the other hand, although rain gauges are more accurate in measuring rainfall intensity at point locations, they lack the ability to reproduce the spatial distribution of rainfall and are also affected by measuring errors. Techniques to merge radar and rain gauge rainfall data can be used to obtain the best estimation of precipitation with the benefits from both types of instruments. Radar-gauge rainfall merging is usually beneficial in terms of improved accuracy and uncertainty reduction, but the merged rainfall product is not error-free and such uncertainty needs to be considered in modelling applications.

This deliverable looks at algorithms to quantify the uncertainty in radar rainfall estimates and in merged radar – rain gauge rainfall estimates. It also investigates how radar rainfall uncertainty can be propagated in models.

The following algorithms are here presented:

a) A logarithmic model is presented to quantify the uncertainty of radar rainfall estimates using rain gauge measurements as a reference, assuming the latter have negligible error.
b) A technique to model and propagate radar uncertainty based on time-variant geo-statistical modelling of ensembles is presented.
c) The formulation of *Ordinary Kriging* (OK) and *Kriging with External Drift* (KED) are presented. These techniques are used to interpolate rain gauge measurements and to merge radar and rain gauge rainfall estimates. Kriging-based techniques have the advantage of offering the kriging variance as a measure of the uncertainty.
d) Two techniques to estimate variograms for KED from radar rainfall estimate are presented.
e) *Kriging for Uncertain Data* (KUD) is presented and discussed as a technique to include spatially and temporally variant rain gauge errors in radar-gauge rainfall merging.
f) To consider radar uncertainty in radar-gauge rainfall merging, instead, a technique named *Kriging with External Drift and Non-Stationary Variance* (KED-NSV) is presented and discussed.
g) An algorithm to produce rainfall ensembles from kriging products is finally presented to propagate rainfall uncertainty in models.

CONTENTS

1 Introduction

1.1 Partners Involved in Deliverable

University of Bristol (UB): Francesca Cecinati (FC), Miguel Rico-Ramirez (MRR).

1.2 Deliverable Objectives

The objective of this deliverable is to provide enhanced algorithms able to quantify uncertainty in radar rainfall measurements. However, since radar rainfall estimates are often merged with rain gauge measurements to improve the accuracy, both the uncertainty in radar rainfall and in merged radar-rain gauge rainfall will be addressed. Six algorithms are here described, to address the following:

1. Modelling of radar rainfall uncertainty,
2. Propagation of rainfall uncertainty in different types of models,
3. Modelling of merged radar-rain gauge rainfall uncertainty,
4. Integration of rain gauge uncertainty in merged radar-gauge rainfall estimations,
5. Integration of radar uncertainty in merged radar-gauge rainfall estimations,
6. Propagation of merged radar-gauge rainfall uncertainty in models.

1.3 Related publications

The material in this deliverable is derived from journal articles, conference proceedings and the PhD work of the first author, produced (or in phase of development) during the QUICS project framework. Technical details, mathematical formulations, and case studies are not reported in this work, but can be found in the related QUICS publications. In particular, the publications relevant to this deliverable are:

- F. Cecinati (2018), Uncertainty estimation and propagation in radar-rain gauge rainfall merging using kriging-based techniques, *PhD thesis*, University of Bristol, Faculty of Engineering, submitted.
- M. A. Rico-Ramirez, G. B. M. Heuvelink, and D. Han (2017), “Representing radar rainfall uncertainty with ensembles based on a time-variant geostatistical error modelling approach,” *J. Hydrol.*, vol. 548, pp. 391–405, DOI: 10.1016/j.jhydrol.2017.02.053.
- F. Cecinati, A. M. Moreno Ródenas, and M. A. Rico-Ramirez (2017), “Integration of rain gauge errors in radar-rain gauge merging techniques,” in 10th World Congress on Water Resources and Environment, pp. 279 – 285.
- F. Cecinati, A. M. Moreno-Ródenas, M. A. Rico-Ramirez, M. ten Veldhuis, J. Langeveld (2017), “Considering rain gauge measurement uncertainty using Kriging for Uncertain Data”, Water Resources Management (in preparation).
- F. Cecinati, A. Wadoux, M. A. Rico-Ramirez, and G. B. M. Heuvelink (2017), “Rainfall estimation using a non-stationary geostatistical model and uncertain measurements,” in 2017 International Symposium Weather Radar and Hydrology, p.163.
- A. M. J-C Wadoux, D. J. Brus, M. A. Rico-Ramirez, G. B. M. Heuvelink, (2017) “Sampling design optimisation for rainfall prediction using a non-stationary geostatistical model”,

Advances in Water Resources, vol. 107, pp. 126-138, DOI: 10.1016/j.advwatres.2017.06.005.

- F. Cecinati, A. C. de Niet, K. Sawicka, and M. A. Rico-Ramirez (2017), "Optimal temporal resolution of merged radar – gauge rainfall for urban applications," *Water*, vol. 9(10), 0762, DOI: 10.3390/w9100762.

1.4 Background

The work in this deliverable has been developed as part of the EU funded project "Quantifying Uncertainty in Integrated Catchment Studies" (QUICS), with the aim of advancing the understanding of rainfall uncertainty, especially as input to hydrological, water quality and integrated models. The objectives of QUICS are to improve the understanding of the different uncertainty sources in catchment studies, develop methods to quantify them, communicate the implications of uncertainty in hydrologic and water quality predictions for decision making, and disseminate knowledge and best practices (Sriwastava and Moreno Ródenas, 2017), in particular to facilitate the application of the EU Water Framework Directive (WFD) (European Community, 2000). The application of the WFD requires many decisions to be taken based on model, such as hydrologic, water quality , urban drainage, and ecological models (Giupponi, 2007; Hering et al., 2010; Quevauviller et al., 2005).

Precipitation estimates are one of the main inputs in many of these models and often represent a significant source of uncertainty. Two main instruments are used to measure rainfall: weather radars, which have a wide aerial coverage and high spatial and temporal resolutions, but do not reach a high accuracy; and rain gauges, which are usually more accurate, but representative of a point in space and lack areal representativeness. Modelling of hydrologic and water quality processes, especially at urban scale, requires high temporal and spatial rainfall resolutions and weather radars are extremely useful tools to meet such model requirements. At the same time, their application in hydrology has been limited by the lower accuracy compared to rain gauges (Berne and Krajewski, 2013). Thus, merging the two sources of rainfall information is a viable way to reach the resolution and accuracy requirements for modelling applications (Berndt et al., 2014; Gabriele et al., 2017; Jewell and Gaussiat, 2015; Nanding et al., 2015). However, a residual uncertainty remains, and very little work has been done on the estimation of radar-gauge merging uncertainty (Erdin et al., 2012). One of the reasons why uncertainty in radar-gauge rainfall merging is hardly studied, is that it is difficult to quantify, since it is cased by many different sources.

On the one hand, radar Quantitative Precipitation Estimation (QPE) is affected by a multitude of errors. Radar QPE is subject to uncertainty due to radar signal anomalous propagation, measurements from non-meteorological echoes, signal attenuation, beam blockage, radar calibration; the relationship between the measured quantity (reflectivity) and the target variable (rainfall intensity) is uncertain as it varies with the rainfall drop size distribution, different atmospheric conditions or different phases of the precipitation. Additionally, there are uncertainties due to the variation of the vertical reflectivity profile or to the beam broadening with distance, etc. (McKee and Binns, 2015; Villarini and Krajewski, 2010a). Several corrections are operationally applied by meteorological offices, especially based on two technological advancements, namely dual-polarization and doppler capabilities of radars, but a residual uncertainty often remains (Harrison et al., 2012, 2000; Overeem et al., 2009; Villarini and Krajewski, 2009).

On the other hand, although several studies on radar uncertainty assume rain gauge uncertainty to be negligible (Ciach et al., 2007; Dai et al., 2014a; Rico-ramirez et al., 2014; Villarini and Krajewski, 2009), this assumption is often not justifiable (Ciach, 2003; Habib et al., 2008; Kitchen and Blackall, 1992; Molini et al., 2005; Villarini et al., 2008). Rain gauges are subject to a variety of systematic and random errors, due to mechanical limitations, wind effects, evaporation, areal representativeness, or data and network management (Bringi et al., 2011; Ciach, 2003; Habib et al., 2004, 2001; Hasan et al., 2014; Lebel et al., 1987; Molini et al., 2005; Nešpor and Sevruk, 1999; Upton and Rahimi, 2003).

This document proposes approaches to quantify the uncertainty associated with radar and rain gauge rainfall measurements, integrate radar and rain gauge uncertainties in the merging process, and evaluate the rainfall estimation uncertainty. The rainfall uncertainty can then be used to analyse how it propagates through natural and urban hydrological models.

2 Radar uncertainty modelling

2.1 Introduction

The use of radar systems for weather surveillance emerged as a consequence of wartime radar technology intensive development. During World War II, the first radars were used to detect enemy targets, emitting radio waves and measuring the bounced signals. Thanks to the invention of the magnetron technology, radars could soon switch to shorter-length microwaves, thus improving their detection resolution and reducing their size (Fabry, 2015). It was thanks to this application that the capability of radars to detect meteorological targets were first observed and studied. In a first moment, the weather applications of radars were just applied to military strategy, but after the end of the second world war, civil applications were developed and operationally used (Whiton et al., 1998a).

The principle underlying weather radar Quantitative Precipitation Estimation (QPE) is that of an active remote sensing instrument: a signal is emitted towards a target, and the echo from the target is measured. In case the radar signal encounters rainfall, a small amount of the emitted signal is scattered back by the hydrometeors (general term that include particles of solid, liquid and mixed precipitation), and can be measured by the radar. The signal received by the radar is proportional to the number and the size of the hydrometeors, therefore to the rainfall intensity. The principal difference between weather radar hydrometeorology and other radar applications is the nature of the target. In radar hydrometeorology, the target is diffused: the radar measures the echo from a multitude of small water targets, impossible to detect individually, but producing an overall measurable echo signal. Therefore, the measured echo depends on the average characteristics of all the particles contained in a volume corresponding to the radar resolution. The state of hydrometeors, solid or liquid, influences the electromagnetic properties of the targets, and the presence of hail and snow needs to be defined to correctly estimate the rainfall intensity. In liquid precipitation, the size of the droplets is proportional to both the reflectivity (Z) and the rainfall intensity (R), and this property can be used to estimate the rainfall intensity measuring the reflectivity. Since the droplet size in any scanned volume can greatly vary, radar hydrometeorology considers the drop size distribution (DSD). However, the reflectivity of the target Z is proportional to the 6^{th} moment of the DSD, while the rainfall intensity R is proportional to the 3.67^{th} moment of the DSD, making the *Z-R* relationship variable (Sauvageot, 1992).

Weather radars work at microwave frequencies. The most commonly used frequency bands are the S-band (2 to 4 GHz), C-band (4 to 8 GHz) and X-band (8 to 12.5 GHz). The higher the frequency, the higher is the spatial resolution that can be achieved, but also the shortest is the range that can be measured, due to a higher level of attenuation (Fabry, 2015; Sauvageot, 1992). For this reason, X-band radars are often used primarily for urban applications, while S-band radars are used mostly when longer distances need to be covered, for example they are operationally used in the USA, while in Europe (including the UK) C-band radars are mainly used operationally. Radar antennas can measure the precipitation along a focused narrow signal beam often around 1-degree resolution. In order to understand where the target is located along the beam range, the time that the signal takes to travel to the target and travel back to the antenna is measured. By pointing the antenna and focusing the radar beam along different directions, radars can measure precipitation on vast areas. In order to measure precipitation as close to the ground surface as possible avoiding

blockage from obstacles, radars operate at different low-elevation angles. Figure 2.1 summarises how a weather radar operationally works.

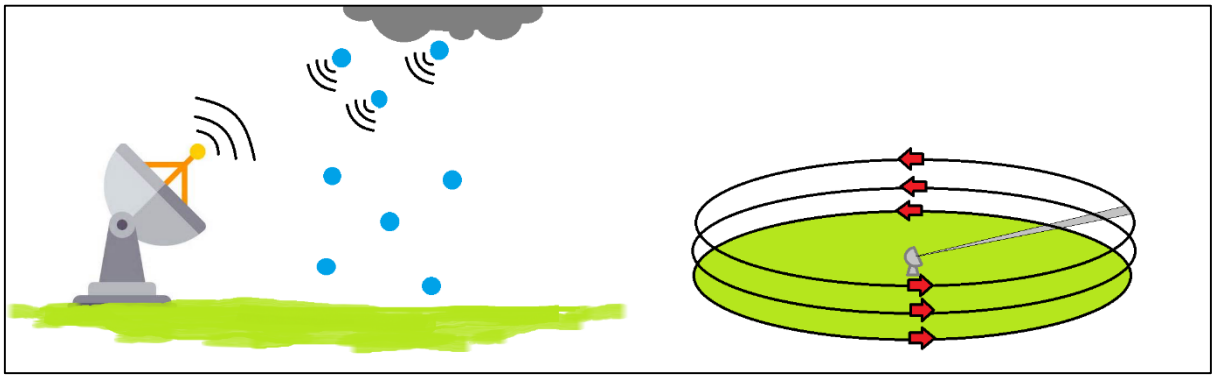

Figure 2.1 – Schematic of a weather radar functioning principle and operation.

Similarly, to the invention of weather radars, it was thanks to the wartime military research and development that a game-changing radar technology was developed: the Doppler radar capabilities. The Doppler effect, i.e. the change of signal frequency due to the movement of the radar target, is exploited to measure the radial velocity of a sensed objects. The use of the Doppler effect was first imagined to detect military target velocity, and only in a second moment it was used for wind speed rainfall measurements. Thanks to the development of the pulse-Doppler technology the range of the target could also be measured and in the 1960's the operational use of pulse-Doppler radars for weather applications was introduced (Whiton et al., 1998b). The use of the doppler capabilities during normal almost-horizontal operations provides information about the drop horizontal (i.e. radial) velocity, that can be critical in reconstructing wind speed, especially in case of severe weather conditions. However, the radar Doppler capabilities can be used also at vertical incidence, i.e. pointing the radar vertically. This type of measurements provides extremely valuable information about the falling velocity of particles, variation of the vertical reflectivity profile, and therefore their DSD and thermodynamic phase can be inferred (Fabry, 2015).

Another critical technology to improve radar QPE is the use of dual-polarisation. Dual-polarisation technology was developed between the 1960's and the 1980's, allowing to drastically reduce many sources of uncertainty in radar precipitation estimates. The emission and measurement of horizontally and vertically polarised microwave signals allows us to retrieve a much larger number of measured parameters, combining the measurements in each polarisation direction. The study of the polarimetric parameters can be used to reconstruct several properties of the target, like, for example, the shape/size of droplets, identification of snow/hail/ground clutter, and overall improvements in signal attenuation and rainfall estimation (Cluckie and Rico-Ramirez, 2004; Doviak, 1983; Hall et al., 2015; Islam et al., 2012a; Rico-Ramirez and Cluckie, 2008; Rico-Ramirez et al., 2005).

It is only in the last decade that most of the national weather radar networks are being updated to full Doppler polarimetric capabilities. Today, radars are one of the most important instruments to measure precipitation. Although they still do not reach the accuracy of most point measurement instruments like rain gauges, the advancements in hardware and software allow radars to estimate spatially distributed precipitation on vast areas, with much higher spatial and temporal resolution compared to satellites. However, there are still several factors that could introduce errors. First of

all, radar quantitative QPE relies on a conversion between the measured reflectivity Z in [mm^6/m^3] and the physical quantity, the rainfall rate R in [mm/h]. The relationship is dependent on the rainfall nature, in particular on drop size distribution (DSD) (Doviak, 1983; Marshall et al., 1947). The adopted Z-R relationships are often calibrated against spatial and temporal average conditions of liquid precipitation, but cannot be tailored to each specific situation and usually fail to correctly estimate extremes or the presence of hail or snow (Austin, 1987; Hasan et al., 2014; Seed et al., 2007). Polarimetric radars can improve the retrieval of the physical quantity R using some of polarimetric parameters (Bringi et al., 2011), but a residual uncertainty remains. Other sources of uncertainty are due to the radar beam propagation that can be partially or totally blocked by obstacles (Friedrich et al., 2007; Joss and Lee, 1995; Westrick et al., 1999), can be deviated by anomalous atmospheric conditions (Moszkowicz et al., 1994; Rico-Ramirez and Cluckie, 2008; Steiner and Smith, 2002), can be attenuated due to heavy precipitation (Atlas and Banks, 1951; Delrieu et al., 2000; Meneghini, 1978; Uijlenhoet and Berne, 2008), and may be subject to beam broadening with range, beam overshooting precipitation, and earth curvature effects, that increase the radar beam height and reduce the resolution at longer ranges (Ge et al., 2010; Kitchen and Jackson, 1993). Ground clutter is another source of error, producing disturbing echoes (Hubbert et al., 2009a, 2009b; Islam et al., 2012c). Similarly, other objects, like wind farms, birds, insects, airplains, or ships can generate dusturbing non-meteorological echoes and other elecromagnetic sources can produce interference. The rainfall rate estimates are often subject to variability of the vertical reflectivity profile (VRP) and to phenomena like the bright band effects, due to the higher reflectivity of the layer in which snow melts into rain that can cause rainfall overestimation up to a factor of 5 if no correction is performed (Austin and Bernis, 1950; Fabry and Zawadzki, 1995; Kirstetter et al., 2013; Qi et al., 2013; Rico-Ramirez and Cluckie, 2007; Smith, 1986; Zhang and Qi, 2010). Errors are also introduced by hardware errors, calibration, spatial and temporal sampling, projection from polar to Cartesian coordinates, and in the averaging operations necessary to obtain the final corrected products (Anagnostou and Krajewski, 1999; Fabry et al., 1994). The list of error sources is long and for an extensive review, the reader is redirected to (Villarini and Krajewski, 2010) and (McKee and Binns, 2015).

Many techniques exist to partially correct different types of errors and are operationally applied by meteorological agencies. As concerns static clutter and blockage from ground, buildings, hills or windfarms, measurements taken in rain free days can be used as a reference (Harrison et al., 2012). Several physics-based techniques can be used to identify anomalous atmospheric conditions, vertical reflectivity profiles, or the freezing level, using atmospheric measurements or numerical weather predictions (NWP), or to identify ground clutter, using digital elevation maps (Gonzalez-Ramirez et al., 2011; Hall et al., 2015; Kirstetter et al., 2013; Kitchen et al., 1994; Krajewski et al., 2006). Errors due to attenuation, solid precipitation, non-meteorological echoes or non-optimal Z-R relationship can be identified considering different doppler and polarimetric parameters, especially using multiple controls with tree diagrams, neural networks and fuzzy logic (Bringi et al., 2001; Dai et al., 2014b; Grecu and Krajewski, 2000; Islam et al., 2012a, 2012b, 2012c; Qi et al., 2013; Rico-Ramirez, 2012). Image analysis can be used to identify speckle and anomalous pixels due to different errors (Harrison et al., 2012; Wesson and Pegram, 2004). Despite meteorological offices invest a great effort in optimally combining these techniques for operational radar QPE correction, a residual uncertainty inevitably affects radar QPE. In processed radar products, the residual uncertainty is due to a mixed combination of the residual uncorrected errors and the processing errors and approximations.

2.2 The logarithmic model

Radar residual errors can be modelled in different ways. Usually, it is recognised that radar residual errors have a bias component and a random component (Ciach et al., 2007). The random component is often modelled as multiplicative (Ciach et al., 2007; Dai et al., 2014a; Villarini and Krajewski, 2009), but sometimes also an additive form is used (Kirstetter et al., 2010).

The model adopted here is additive in the log-transformed domain, thus it is multiplicative in the original domain:

$$10\log(P) = 10\log(R) + \delta \quad (1)$$

where P is the true rainfall, R is the radar QPE, δ is the residual error that is subsequently modelled to contain a bias correction as well, and the log operation refers to a logarithm with base 10. The model is consistent with previous research, in particular with the model adopted in the REAL (radar ensemble generator using LU decomposition) method by Germann et al., (2009). The advantage of such a form is that the residual errors have an almost Gaussian probability distribution, which is characterised only by the mean $\mu(\delta)$, the standard deviation $\sigma(\delta)$, and the spatial correlation. Figure 2.2 is an example of the probability distribution of radar residual errors calculated with an additive, a multiplicative and a logarithmic form, using data from the UK Environment Agency rain gauges and the UK Met Office radar estimates for one year in 2008. In the phase of error estimation, the true rainfall P is approximated with rain gauge measurements G, and the residual errors δ are defined as follows:

$$\delta = 10\log(G) - 10\log(R) \quad (2)$$

$$\mu(\delta) = E\{\delta\} \quad (3)$$

$$\sigma(\delta) = \sqrt{E\{(\delta - \mu(\delta))^2\}} \quad (4)$$

where $E\{\}$ is mathematical expectation, approximated with the mean. Figure 2.2 also reports the values of Skewness, Kurtosis (Joanes and Gill, 1998), and approximation of negentropy (Hyvärinen and Oja, 2000), as indicators of Gaussianity. All of the indicators should tend to zero for a Gaussian distribution.

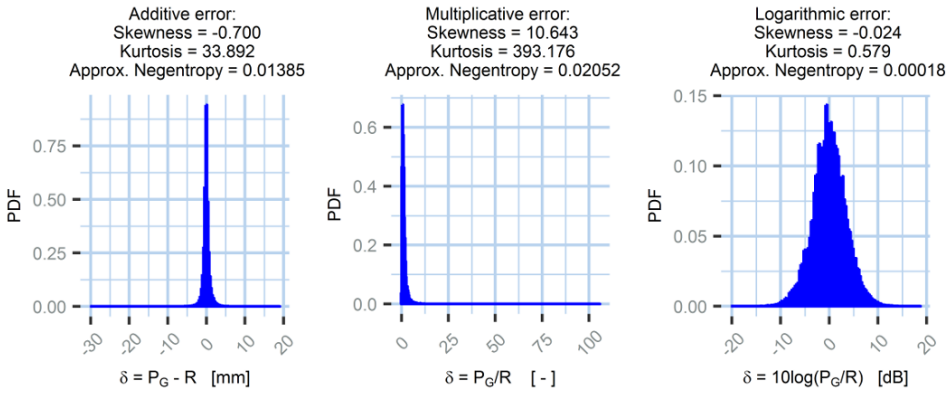

Figure 2.2 - Probability distribution associated to radar errors modelled in an additive form, in a multiplicative form, and in a logarithmic form.

2.3 Modelling the spatial correlation

The residual errors must also be defined in terms of correlation characteristics. Literature shows that temporal autocorrelation of residual errors at hourly time steps is usually limited (Kirstetter et al., 2010; Rico-Ramirez et al., 2015; Wheater et al., 2000), therefore the attention in this work is focused on the spatial correlation structure. Often, the spatial correlation characteristics are depicted with a variance-covariance matrix C, describing the covariance between each pair of errors $\delta(x_i)$ and $\delta(x_j)$ (Germann et al., 2009):

$$C\big(\delta(x_i)\,,\delta(x_j)\big) = E\big\{(\delta(x_i)-\mu_i)\big(\delta(x_j)-\mu_j\big)\big\} \quad i,j=1,\dots,N \tag{5}$$

where the expected value is in practice calculated on time series. Parameters μ_i and μ_j, short notation for $\mu\big(\delta(x_i)\big)$ and $\mu\left(\delta\big(x_j\big)\right)$, are the mean of the residual error values $\delta(x_i)$ and $\delta(x_j)$, also calculated from the time series. The variance-covariance matrix may become unstable when the number of measuring points (N) is large. In fact, it must be positive-definite, which an empirical variance-covariance matrix might not be. Moreover, its inversion is computationally demanding for large *N* and may lead to numerical instabilities when the matrix is near-singular. It is also not suitable for time-variant calculation of error characteristics, because it calculates the expected values on time series, assuming stationarity of the characteristics in time (Le Ravalec et al., 2000). In reality, radar errors are neither stationary in time nor space, because they are dependent on the rainfall rate and on temporary conditions like attenuation or bright band phenomena, variability of the parameters *a* and *b* of the *Z-R* relationship (where $Z=aR^b$) due, for example, to convective storms, drizzle, snow, or hail, and so on.

The spatial correlation characteristics of the residual errors can be represented through variograms. Variograms describe the variance as a function of the separation distance d (Cressie, 1993):

$$\gamma(d) = \frac{1}{2}E\{(\delta(x)-\delta(x+d))^2\} \tag{6}$$

An empirical variogram is calculated from the observations, binning the observation point distances in regular intervals. It requires an assumption of spatial intrinsic stationarity of the field (Cressie, 1993). Empirical variograms are then fitted with theoretical variogram functions. Variograms describe the spatial characteristics of the residual errors through three parameters, the range

parameter h, the sill c, and the nugget c_0. The most common functions to fit empirical variograms are:

$$exponential: \quad \hat{\gamma}(d) = \begin{cases} c_0 + c\left(1 - \exp\left(-\frac{3d}{h}\right)\right) & d > 0 \\ 0 & d = 0 \end{cases} \tag{7}$$

$$Gaussian: \quad \hat{\gamma}(d) = \begin{cases} c_0 + c\left(1 - \exp\left(-\frac{3d^2}{h^2}\right)\right) & d > 0 \\ 0 & d = 0 \end{cases} \tag{8}$$

$$spherical: \quad \hat{\gamma}(d) = \begin{cases} c_0 + c\left(1.5\left(\frac{d}{h}\right) - 0.5\left(\frac{d}{h}\right)^3\right) & 0 < d \leq h \\ c + c_0 & d > h \\ 0 & d = 0 \end{cases} \tag{9}$$

The fitting is usually performed with a weighted least square method that uses a weight in the form N_o/d^2, where N_o is the number of available observations per distance bin and d is the distance (Cressie, 1985; Zhang and Eijkeren, 1995). Variograms have the advantage of being fast to calculate and easy to use.

3 Propagating radar uncertainty

3.1 Introduction

When radar QPE is used for hydrological applications, the estimation of its uncertainty and the assessment of uncertainty propagation in hydrological models is essential (Berne and Krajewski, 2013; Pappenberger and Beven, 2006; Schröter et al., 2011). An effective method to model uncertainty in radar QPE for hydrological model applications is the use of radar ensembles, which can easily be applied to hydrological models to assess residual error propagation in the model output (AghaKouchak et al., 2010; Germann et al., 2009; Villarini et al., 2009). This approach is based on estimating the residual errors in radar QPE as a comparison with reference ground measurements, like those provided by rain gauges, used as an approximation of true rainfall. The observed radar QPE residual errors are then used to build an error model describing the statistical characteristics of the errors; knowing the statistical characterisation of the radar QPE residual errors, a large number of alternative possible realisations of the observed rainfall fields, constituting an ensemble, can be computed. The uncertainty propagation through models can be estimated by observing the resulting spread after feeding a model with multiple ensemble members.

Several methods for radar ensemble generation are proposed in the literature, of which many are based on the computation of the error covariance matrix (AghaKouchak et al., 2010; Dai et al., 2014; Germann et al., 2009; Kirstetter et al., 2015; Villarini et al., 2014, 2009). The covariance matrix approach is a powerful and well-tested method that uses the covariance matrix decomposition to condition uncorrelated random normal deviates, in order to simulate alternative error components for the ensemble. A well-formulated example is the REAL generator proposed by Germann et al., (2009). However, it has some limitations when the number of rain gauges is large, because the covariance matrix calculation becomes computationally demanding and the decomposition unstable. In addition, ensemble error components are generated only at ground measurement points, needing subsequent interpolation that alters the spatial structure and introduces significant smoothing problems. Finally, in the calculation of the covariance matrix the spatial non-stationarity of the errors is captured assuming temporal stationarity. In other words, although the covariance approach reproduces the covariances between the errors at each rain gauge location, it assumes temporal stationarity of errors. Radar errors are non-stationary both in space and in time, but with a limited number of observations it is necessary to consider one of the two dimensions stationary in order to have enough observation points to calculate statistics. In this work, the possibility to model radar errors that are non-stationary in time and stationary in space is explored. The variability in space observed at ground measurement points is partially reproduced using conditional simulations for the error component generation.

3.2 Spatial vs temporal variability of radar error characteristics

This document proposes an ensemble generation approach aiming at reducing the computational load, improving stability, eliminating the need for error component interpolation, and producing time-variant residual error characterisation. This approach allows us to better capture time-dependent characteristics of residual errors, due for example to temporary conditions like the presence of bright band, hail or attenuation. The spatial characterisation of the residual errors is based on the use of variograms fitted with parametric models, which have the advantage of using only a limited number

of variogram parameters (i.e. range, sill, and nugget), for full description and of being calculable with short time series. In comparison with the covariance matrix approach, the variogram approach constitutes a compromise, by exchanging temporal stationarity of the residual errors with spatial stationarity. In fact, although this method is able to reproduce the variability in error statistics over time, it considers errors stationary in space in the study area. However, the data from the UK Environment Agency rain gauges and the UK Met Office radar estimates for one year in 2008 are here used to understand which dimension has the most variability. The coefficient of variation is calculated for both mean and standard deviation. As reported in Table 3.1, the absolute value of the coefficient of variation calculated over time is slightly higher for the mean, and clearly higher for the standard deviation. This means that assuming stationarity over space introduces a lower error than assuming stationarity over time.

Table 3.1 - Coefficient of variation (unitless) for the mean and the variance, calculated over space and over time:

	CV over space	**CV over time**
$\boldsymbol{\mu(\delta)}$	8.272	-8.689
$\boldsymbol{\sigma(\delta)}$	0.090	0.336

Furthermore, the error components are generated in a conditional way, so that the observed errors are reproduced and that all other simulated error points are conditioned on the observed ones. Although the mean and variance adjustment partially alters the reproduction of the observed errors, the geo-statistical approach still contributes to reproduce the spatial variability of errors.

3.3 Error components for radar ensemble members

Error measurements are obtained using quality checked rain gauge data as an approximation of true rainfall. In order to generate error components with the desired mean, variance and variogram characteristics, conditional simulations are used. The method presented by Delhomme (1979) is selected, due to its calculation speed and numerical stability, which makes it suitable for unsupervised applications to long time series. The method is based on the following steps:

a) For each time step t, an arbitrary number K of non-conditional simulations $\tilde{\delta}_{NC,i}(t,x)$ are generated, where $i = 1, \dots, K$. The method used here is the sequential simulation implemented in the *gstat R* package (Pebesma, 2004).

b) The observed errors at time t are interpolated with kriging, obtaining the interpolated fields $\delta_k(t,x)$.

c) The values of the non-conditional simulations $\tilde{\delta}_{NC,i}(t,x)$ at observation locations are kriged to obtain the fields $\delta_{k_{NC,i}}(t,x)$.

d) The conditional simulations $\tilde{\delta}_i(t,x)$ are obtained as follows:

$$\tilde{\delta}_i(t,x) = \delta_k(t,x) - \tilde{\delta}_{NC,i}(t,x) + \delta_{k_{NC,i}}(t,x) \quad (10)$$

Due to the logarithmic formulation, errors cannot be calculated when the rain gauges do not record rainfall. If no rain gauge records rainfall, unconditional simulations are used.

Important features of the generated fields are that they are Gaussian (in the logarithmic domain), are characterised using the observed variogram, and are conditioned on the observed errors. In addition, compared with the fields generated through the REAL method, the generated fields are already gridded fields and do not require any interpolation that tends to smooth the spatial features of the error components. In fact, an interpolation uses the kriging mean, i.e. the most probable value for each pixel. Instead, in the methodology applied here, at each pixel is assigned a different possible realisation for each ensemble member, in agreement with the conditional distribution.

3.4 Radar ensemble generation

Following the error model, the i^{th} simulated error field $\tilde{\delta}_i(t,x)$ can be used to produce the i^{th} simulated QPE $\tilde{P}_i(t,x)$ for each time step t:

$$10\log\left(\tilde{P}_i(t,x)\right) = 10\log(R(t,x)) + \tilde{\delta}_i(t,x) \tag{11}$$

Since the logarithm of the radar field $R(t,x)$ cannot be calculated when a pixel is zero, pixels that do not record rainfall are not used and the zero values are re-introduced in the ensemble members in a second moment, after a mean and variance adjustment passage. In fact, the structure of the model is such that the new error members are Gaussian in the logarithmic domain, but the back-transformation to the final field $\tilde{P}$ gives a different weight to positive and negative deviations, shifting the overall mean toward higher values and increasing the variance.

3.5 Mean and variance re-adjustment

The bias introduced by a logarithmic back-transformation (Erdin et al., 2012) is not discussed by Germann et al., (2009), when the same error model is applied to the REAL ensemble generator. In addition, the new simulated error components are added to the radar field, which already contains errors, inflating the overall variance (Pegram et al., 2011). In order to have rainfall fields consistent with the observed approximation of true rainfall from the rain gauges, the mean and the variance need to be re-adjusted. In this work a linear adjustment is used at each time step t to re-adjust mean and variance of the generated ensemble members, without modifying the spatial characteristics so carefully reproduced:

$$\tilde{P}_{new,i} = \frac{\sigma_G}{\sigma_{\tilde{P}_{orig}}}\left(\tilde{P}_{orig,i} - m_{\tilde{P}_{orig}}\right) + m_G \tag{12}$$

where $\tilde{P}_{new,i}$ is the new i^{th} ensemble member after correction, $\tilde{P}_{orig,i}$ is the original i^{th} ensemble member, $\sigma_{\tilde{P}_{orig}}$ is the standard deviation of all original ensemble members across all the rain gauge measuring locations, $m_{\tilde{P}_{orig}}$ is the average of all the original ensemble members at the rain gauge measuring locations, σ_G is the standard deviation of the rain gauge measurements, m_G is the mean of the rain gauge measurements.

It must be noted that the adjustment is not forcing each ensemble member to reproduce the mean of the rain gauge values. Instead, the adjustment forces the overall ensemble mean to tend to the true value, represented by the rain gauge measurements. This is justified by the definition of ensemble as a representation of the rainfall uncertainty due to the radar, therefore it should convey

how much from the true value the radar data can deviate, where the true value is represented by the ensemble mean and the deviations by the single ensemble members. Similarly, the adjustment does not force the ensemble standard deviation at each point, but it corrects the spatial standard deviation of each ensemble member, in order to re-adjust the exponential stretch and avoid unrealistically high intensity values. The adopted solution is an approximation, but it is effective in obtaining possible realistic alternative rainfall fields.

4 Merging radar and rain gauge rainfall

4.1 Introduction

Hydrology, especially at urban scale, requires accurate rainfall data with high temporal and spatial resolutions (Schilling, 1991). Ideally the availability of very dense high-accuracy rain gauge networks could provide the necessary rainfall information, but rarely national and regional networks meet the required gauge density, and it is necessary to integrate the measurements with additional data (Berne et al., 2004). Weather radars provide a full aerial coverage and commonly reach a 5-minute temporal resolution and 1-km spatial resolution, sufficient for urban applications in medium-large urban areas, but hardly offer the required accuracy (Einfalt et al., 2004). It is recognised that merging radar rainfall data with rain gauge measurements allows to maintain spatial coverage and the resolution of radar data and improve the accuracy of the estimates, (Berndt et al., 2014; Creutin et al., 1988; Gabriele et al., 2017; Goudenhoofdt and Delobbe, 2009; Jewell and Gaussiat, 2015; Krajewski, 1987). The idea of using accurate ground measurements to correct radar QPE is not new. Simple bias adjustments are operationally applied to adjust major radar QPE deviations (Harrison et al., 2000; Overeem et al., 2013) and in the last 30 years several geostatistical approaches have been presented. Krajewski, (1987), and Creutin et al., (1988), proposed a co-kriging (CK) approach to interpolate rainfall measurements at unmeasured locations, using both rain gauge and radar measurements at rain gauge locations, using different weights. However, the co-kriging approach does not take into account the different strengths and the different weaknesses of the two rainfall measuring systems. Co-kriging uses radars only at rain gauge locations, limiting the advantage of having a measuring system that can observe the spatial structure of rainfall. Kriging with External Drift (KED), although widely known in the geostatistical field for a long time (Chiles and Delfiner, 1999; Cressie, 1993; De Marsily, 1986) has become a widely recognised radar-gauge merging method for rainfall measurements more recently (Delrieu et al., 2014; Grimes et al., 1999; Haberlandt, 2007; Velasco-Forero et al., 2004, 2009). The principle of KED is to interpolate rain gauge measurements, using a linear function of the radar QPE to model the process mean. In this way, the rainfall absolute values are driven primarily by the rain gauge measurements, while the spatial distribution of rainfall is drifted by the radar QPE. In a similar way, Sinclair & Pegram, (2005), use conditional merging (CM) to exploit the spatial distribution of rainfall observed by radar QPE to modify the rain gauge interpolation. In particular, CM uses the deviation from the interpolation of radar measurements at rain gauge locations to spatially correct the rain gauge interpolation. A more advanced technique proposed by Todini, (2001), merges a Bayesian approach with a data assimilation one, using a Kalman filter to integrate radar and rain gauge measurements. Overall, several studies have been carried out to compare different radar-gauge rainfall merging techniques (Goudenhoofdt and Delobbe, 2009; Jewell and Gaussiat, 2015; Li and Heap, 2011; McKee and Binns, 2015; Nanding et al., 2015). KED emerges as a robust and simple technique to improve radar rainfall estimation accuracy, and for this reason is particularly interesting for operational applications (Sideris et al., 2014). Other methods that perform comparably well, usually require considerably more computational effort, making use of large covariance matrices or Monte Carlo methods (Scheidegger and Rieckermann, 2014; Todini, 2001) and this high computational cost is an obstacle for their operational usage, especially for large areas, or for long time series. For these reasons, in this document KED is used and analysed. It must be noted that the mentioned techniques perform the radar-gauge merging in space, but consider each time step independently. Geostatistical

methods do exist to perform merging with spatio-temporal kriging (Sideris et al., 2014; Snepvangers et al., 2003; Spadavecchia and Williams, 2009), but the methodologies are more complex and are not discussed in this dissertation. However, the techniques presented in this work are modular and can be applied or adapted to different kriging-based techniques, thus can be adapted to spatio-temporal kriging as well.

4.2 Ordinary Kriging (OK)

Although Ordinary Kriging (OK) is not a merging technique, it is here illustrated as the basis of most kriging-based merging techniques and kriging-based algorithms used in this deliverable. The term "kriging" originates from the name of the South African Statistician Danie G. Krige, that first introduced the concept of distance-weighted averaging for spatial interpolation of mining samples (Krige, 1952). The use of the term "kriging" has been introduced by Matheron (1963), who first formalised the technique (Cressie, 1990). In ordinary kriging, the prediction in each point is calculated as the weighted average of the available measurements:

$$\hat{P}(x_0) = \sum_{\alpha=1}^{n} w_\alpha \cdot G(x_\alpha) \tag{13}$$

where $\hat{P}(x_0)$ is the estimated rainfall in a generic point x_0, $G(x_\alpha)$ are the measured values at rain gauge locations x_α, n is the number of observations, and w_α are the kriging weights, estimated following two principles:

1) The prediction has to be unbiased,
2) The variance of the prediction error has to be minimised.

The two principles result in the kriging system:

$$\begin{cases} \sum_{\alpha=1}^{n} w_\alpha(x_0) = 1 \\ \sum_{\alpha=1}^{n} w_\alpha(x_0) \cdot C(x_\alpha - x_\beta) + \mu = C(x_\beta - x_0) \quad \beta = 1, \dots, n \end{cases} \tag{14}$$

where x_α and x_β are generic rain gauge locations, and μ is the Lagrange parameter (Cressie, 1993). $C(d)$ is a covariance function, defining the covariance of the process between two measurements at distance d. The kriging system in Equation 14 can be written in matrix form:

$$\boldsymbol{W} = \boldsymbol{C}^{-1} \cdot \boldsymbol{D} = \begin{bmatrix} w_1 \\ w_2 \\ \vdots \\ w_n \\ \mu \end{bmatrix} = \begin{bmatrix} C_{11} & C_{12} & \dots & C_{1n} & 1 \\ C_{21} & C_{22} & \dots & C_{2n} & 1 \\ \vdots & \vdots & \ddots & \vdots & \vdots \\ C_{n1} & C_{n2} & \dots & C_{nn} & 1 \\ 1 & 1 & \dots & 1 & 0 \end{bmatrix}^{-1} \cdot \begin{bmatrix} C_{10} \\ C_{20} \\ \vdots \\ C_{n0} \\ 1 \end{bmatrix} \tag{15}$$

where $\boldsymbol{W}$ is the vector of the kriging weights and the Lagrange parameter, $\boldsymbol{C}$ is the covariance matrix, C_{ij} is the short notation for $C(x_i - x_j)$ representing the covariance function applied to the distance between two generic rain gauges, $\boldsymbol{D}$ is the vector of the covariance function applied to the distances between each rain gauge and the prediction point x_0, where C_{i0} is the short notation for $C(x_i - x_0)$.

The kriging variance $\sigma^2(x_0)$ after optimisation is calculated as follows:

$$\sigma^2(x_0) = c - \sum_{\alpha=1}^{n} w_\alpha(x_0)\, C(x_\alpha - x_0) - \mu = c - \boldsymbol{W} \cdot \boldsymbol{D} \tag{16}$$

4.3 Kriging with External Drift (KED)

While the process in ordinary kriging assumes a stationary mean, in KED the rainfall process mean is assumed non-stationary in space:

$$P(x) = m(x) + \sigma \cdot \epsilon(x) \tag{17}$$

where $m(x)$ is the mean (or spatial trend), σ is the residual standard deviation, and $\epsilon(x)$ is a zero-mean, unit variance, normally distributed, spatially correlated, second-order stationary random process (Webster and Oliver, 2001). In KED, the mean of the process is often expressed as a linear function of explanatory covariates (for this reason the method is also referred to as *regression kriging*):

$$m(x) = \sum_{k=0}^{K} \alpha_k \cdot f_k(x) \tag{18}$$

where α_k are regression coefficients, $f_k(x)$ are a certain number K of covariates in any estimation location x. Assuming $f_0(x) = 1$, the coefficient α_0 is an intercept. Generally, the mean is assumed as a function of only one covariate, which in this case is the radar QPE:

$$m(x) = \alpha_0 + \alpha_1 R(x) \tag{19}$$

where $R(x)$ is the radar rainfall estimate in x, whereas α_0 and α_1 are a linear coefficients to be determined (Cressie, 1993). This changes the kriging system to define the kriging weights:

$$\begin{cases} \sum_{\alpha=1}^{n} w_\alpha(x_0) = 1 \\ \sum_{\alpha=1}^{n} w_\alpha(x_0) \cdot C(x_\beta - x_\alpha) + \mu_1 + \mu_2 \cdot r(x_\beta) = C(x_\beta - x_0) \quad \beta = 1, \dots, n \\ \sum_{\alpha=1}^{n} w_\alpha(x_0) \cdot R(x_\alpha) = R(x_0) \end{cases} \tag{20}$$

where μ_1 and μ_2 are two Lagrange parameters, and $R(x_i)$ represent the radar estimate in x_i. The system in matricial form becomes:

$$\boldsymbol{W} = \boldsymbol{C}^{-1} \cdot \boldsymbol{D} = \begin{bmatrix} w_1 \\ w_2 \\ \vdots \\ w_n \\ \mu_1 \\ \mu_2 \end{bmatrix} = \begin{bmatrix} C_{11} & C_{12} & \dots & C_{1n} & 1 & R_1 \\ C_{21} & C_{22} & \dots & C_{2n} & 1 & R_2 \\ \vdots & \vdots & \ddots & \vdots & \vdots & \vdots \\ C_{n1} & C_{n2} & \dots & C_{nn} & 1 & R_n \\ 1 & 1 & \dots & 1 & 0 & 0 \\ R_1 & R_2 & \dots & R_n & 0 & 0 \end{bmatrix}^{-1} \cdot \begin{bmatrix} C_{10} \\ C_{20} \\ \vdots \\ C_{n0} \\ 1 \\ R_0 \end{bmatrix} \tag{21}$$

where R_i is short for $R(x_i)$ and it is the radar measurement at rain gauge location x_i, while R_0 is $R(x_0)$, the radar measurement in the prediction location x_0. The kriging variance $\sigma^2(x_0)$ after optimisation is calculated as follows:

$$\sigma^2(x_0) = c - \sum_{\alpha=1}^{n} w_\alpha(x_0)\, C(x_\alpha - x_0) - \mu_1 - \mu_2 = c - \boldsymbol{W} \cdot \boldsymbol{D} \tag{22}$$

The kriging variance represents the uncertainty associated to the kriging rainfall estimation.

4.4 Variogram calculation

In order to use kriging interpolation methods, it is necessary to define a covariance function. The covariance function $C(d)$ is related to the variogram function $\gamma(d)$ as follows:

$$C(d) = c + c_0 - \gamma(d) \tag{23}$$

where c is the sill parameter and c_0 is the nugget, both estimated together with the variogram function. Empirically, the variogram is usually calculated observing the variance between all the available measurement points as a function of their distance, as presented in Section 2. However, in KED there are two issues to consider:

1. The number of available rain gauges may be limited, and their resolution highly variable, therefore a reliable time-variant variogram calculation based on ground measurements can be difficult to calculate.
2. In KED, the variogram needs to be calculated on rainfall residuals, rather than on the rainfall field itself (Cressie, 1993).

While the first problem is based on a purely practical problem that may or may not be present, according to the specific case study, the second problem is more intrinsic in the KED formulation. In fact, the rainfall residuals, calculated as the difference between the rainfall process and the drift, are necessary to calculate the variogram, but are unknown, as both the rainfall estimation and the drift need to be determined. One possible approach is to make a first KED estimation, then iteratively repeat the KED estimation updating both the rainfall field and the drift until the estimations converge. However, this approach is time consuming and computationally intense, therefore is usually avoided. In this work two approaches are presented to address both the issues illustrated before, basing the variogram calculation on the radar QPE. Although the radar QPE is considered less accurate than rain gauge measurements, in this work they are considered accurate enough to estimate a reliable variogram, and have the advantage of representing the rainfall spatial variability much better than sparse point measurements.

4.4.1 Estimating a variogram with a radar subset

The first approach is to use a subset of the radar QPE to have a first estimation of the rainfall variogram. The number of radar QPE pixels is in general much higher than the number of available rain gauges, even when only sparse rain occurs. Once a rainfall variogram is estimated, it can be used to interpolate the rain gauges, and estimate the residual as the difference between the rain gauge interpolation and the radar QPE. The methodology is based on four-passages:

1. The rainfall empirical variogram is estimated using a subset of the wet radar pixels, following Equation 6. In particular, all wet radar pixels can be used, if not much rainfall is recorded, otherwise variogram estimation can be based on a random subset of the available wet pixels, to limit the computational load.
2. Ordinary kriging is performed on the available rain gauges, obtaining the interpolated field $\hat{P}_{OK}(x)$.
3. The residuals $y(x)$ are estimated as the difference between the $\hat{P}_{OK}(x)$ field and a linear function of the radar estimate:

$$y(x) = \hat{P}_{OK}(x) - (\widehat{\alpha_0} + \widehat{\alpha_1} R(x)) \tag{24}$$

   where $\widehat{\alpha_0}$ and $\widehat{\alpha_1}$ are estimated fitting a linear regression between the $\hat{P}_{OK}(x)$ field and the radar QPE $R(x)$.
4. An empirical variogram is calculated as in point 1, using the residual field $y(x)$ instead of the radar field.

4.4.2 Fast Fourier Transform (FFT)

The method proposed above has the limitation of being dependent on the radar QPE subsample selected, and being relatively computationally intense. An alternative is to derive the variogram from

the entire radar QPE field, using a Fast Fourier Transform (FFT) approach. The derivation is illustrated in the work from Marcotte, (1996), and results in the following formulation to calculate the FFT-derived variogram $\gamma_{FFT}(d)$:

$$\gamma_{FFT}(d) = Re\left(\frac{FFT^{-1}(\boldsymbol{V_2^*} \cdot \boldsymbol{I} + \boldsymbol{I}^* \cdot \boldsymbol{V_2} - 2\boldsymbol{V} \cdot \boldsymbol{V}^*)}{2FFT^{-1}(\boldsymbol{I} \cdot \boldsymbol{I}^*)}\right) \quad (25)$$

where all the arithmetic operations are computed element by element, $\boldsymbol{V}$ is the FFT of the radar QPE matrix, $\boldsymbol{V_2}$ is the FFT of the square of the radar QPE matrix (squared element by element), $\boldsymbol{I}$ is the FFT of an identity matrix with the same size of the QPE matrix, the * operator indicates the conjugate, and the $Re(-)$ operation indicates the real part. The QPE matrix needs to be padded with zeros to reach a square with the side size, in pixels, equal to a power of two. Similarly, all the missing data in the QPE matrix need to be substituted with zeros.

Besides the computational speed, another great advantage of the variogram calculated this way is that it is bi-dimensional and allows to consider anisotropy. However, on the counter side, the FFT approach is very sensitive to missing data, and cannot be used if part of the rectangular domain is missing, for example if the rainfall field is cropped on a watershed or on administrative borders. Figure 4.1 illustrate an example of bi-dimensional variogram calculated with the FFT approach over northern England, for two example time steps in 2016, one representing a stratiform event in March, and one representing a convective event in June.

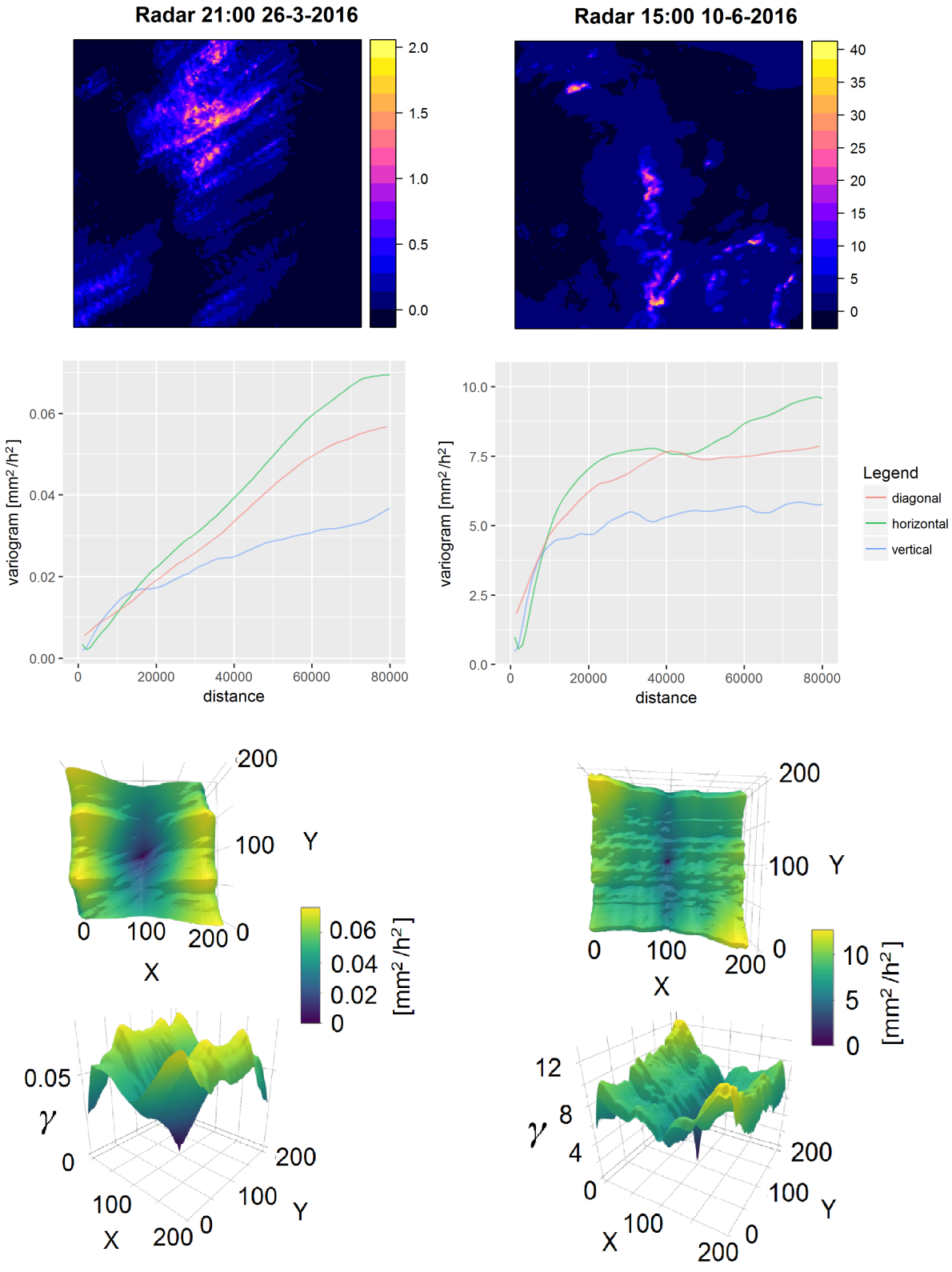

Figure 4.1 - Example of bi-dimensional variograms calculated for two time-steps in 2016, a stratiform event in March and a convective one in June, over the north of England.

5 Integration of rain gauge errors in radar-gauge merged products

One of the advantages of kriging-based merging methods is that the estimation of the kriging variance provides a starting point to estimate rainfall uncertainty. However, the standard kriging formulation allows to consider only a spatially uniform measurement uncertainty. In fact, the use of a nugget effect in the geostatistical model can represent measurement errors, but does not allow to consider a different uncertainty for each measurement point (Clark, 2010; Cressie, 1993). In some applications, rain gauge uncertainty is assumed to be small enough to be neglected (A. AghaKouchak et al., 2010; Ciach et al., 2007; Dai et al., 2014a; Germann et al., 2009; Rico-Ramirez et al., 2015; Villarini and Krajewski, 2009). This can be done when the accumulation time is not too small (Ciach et al., 2007) and when rain gauges are accurate and their data is correctly managed and calibrated (Habib et al., 2004, 2008; Molini et al., 2005; Nešpor and Sevruk, 1999; Sevruk, 1996). Unfortunately, in many operational networks the importance of accurate rainfall data and of data quality control can be underestimated; budget and best practice knowledge can be limiting factors in a correct rain gauge network management. In these cases, the accuracy of rain gauges can drastically drop and the uncertainty associated with the measurements cannot be neglected anymore (Steiner et al., 1999). Additionally, frequently rain gauge networks are not dense enough to capture the spatial characteristics of rainfall in urban applications (Peleg et al., 2013; Villarini et al., 2008) and integrating different rain gauge networks, with different accuracy characteristics is often necessary.

The uncertainty in rain gauge rainfall data is due to different error sources (Upton and Rahimi, 2003). Rain gauges are affected by predictable errors due, for example, to wind under-catch (Nešpor and Sevruk, 1999). For tipping bucket devices, partial filling of the bucket and delayed tipping at low intensities, or limits in the mechanical tipping at high intensities are additional problems (Habib et al., 2001; Molini et al., 2005). These errors can be modelled and partially corrected with calibration. Rain gauges are also affected by random errors, which cannot be predicted or deterministically modelled (Ciach, 2003). Another problem in the use of rain gauges as a ground reference is that they are representative of points, while they are often used as aerial reference, generating point-to-area errors (Bringi et al., 2011; Habib et al., 2004; Hasan et al., 2014; Lebel et al., 1987). In addition, poor data management can introduce additional errors, like missed recording of cleaning operations or maintenance, mismatch of temporal and spatial references, or absence of metadata on calibration and processing, which introduce unknown errors (Molini et al., 2005). In this deliverable, a model is proposed to integrate time- and space-variant measurement point errors in the rainfall uncertainty quantification.

The integration of point measurement uncertainty in kriging has been studied in literature. A solution in case of homoscedasticity is the use of the nugget effect (Clark, 2010; Cressie, 1993), but it assumes that all rain gauge measurements are characterised by the same uncertainty. However, the magnitude of measurements errors can greatly vary in space (Stein, 1999). De Marsily (1986) formulated a method to handle different variances for different point measurement errors, called Kriging for Uncertain Data (KUD). The formulation was further developed by Mazzetti and Todini (2009). KUD can be applied to different kriging-based algorithms, including ordinary kriging (OKUD) and KED (KEDUD). The formulation in this work is an equivalent simplified version of the one presented by Mazzetti and Todini (2009).

5.1 Kriging for Uncertain Data (KUD)

The most diffused geostatistical method to consider measurement errors in kriging interpolations is to use a nugget effect in the geostatistical model (Clark, 2010; Cressie, 1993). Including measurement errors in the nugget implies an assumption of homoscedasticity, i.e. all the different measurements from all the different measuring points are affected by the same uncertainty. However, there are two main reasons why this model cannot be applied to rain gauge interpolation: 1) rainfall measurement uncertainty is known to be dependent on the rainfall intensity, which is highly variable in space and time (Ciach, 2003; Habib et al., 2001); 2) different types of rain gauges are affected by different error models.

De Marsily, (1986), proposed a method named Kriging for Uncertain Data (KUD) able to consider a different measurement error for each measuring point and Mazzetti and Todini (2009) perfected the formulation. The formulation proposed in this work is equivalent to the one of Mazzetti and Todini (2009). Using a covariance function, the nugget effect affects only measurements at distance equal to zero. In facts, combining Equations 7, 8, and 9 with Equation 23, the following covariance functions are obtained:

$$exponential: \quad \hat{\gamma}(d) = \begin{cases} c \cdot \exp\left(-\frac{3d}{h}\right) & d > 0 \\ c_0 + c & d = 0 \end{cases} \tag{26}$$

$$Gaussian: \quad \hat{\gamma}(d) = \begin{cases} c \cdot \exp\left(-\frac{3d^2}{h^2}\right) & d > 0 \\ c_0 + c & d = 0 \end{cases} \tag{27}$$

$$spherical: \quad \hat{\gamma}(d) = \begin{cases} c - c\left(1.5\left(\frac{d}{h}\right) - 0.5\left(\frac{d}{h}\right)^3\right) & 0 < d \leq h \\ 0 & d > h \\ c_0 + c & d = 0 \end{cases} \tag{28}$$

This means that the only elements affected by the nugget effects are the covariance matrix diagonal elements in Equations 15 and 21, for OK and KED respectively. The elements of the diagonal can therefore be modified one by one, adding the estimated error for each rain gauge:

$$\begin{cases} C_{ii} = C(0) + c_{0_i} \\ C_{ij} = C(x_i - x_j) \quad i \neq j \end{cases} \tag{29}$$

where the error c_{0_i} are calculated for each rain gauge, according to the available information on its accuracy and its type.

5.2 Rain gauge error modelling

The most common type of rain gauges is tipping bucket rain gauges (TBRs). The random errors for TBRs can be modelled according to the model by Ciach, (2003). The standard error is calculated as:

$$\sigma_{err}(T_1, P_T) = e_0(T_1) + \frac{P_0(T_1)}{P_T} \tag{30}$$

where P_T is the rainfall intensity at accumulation $T = T_1$ minutes, while $e_0(T_1)$ and $P_0(T_1)$ are coefficients dependant on the accumulation time. Figure 6 in Ciach's work (Ciach, 2003) shows the errors of the rain gauge data. Using this figure, we derived an approximated analytical formulation where T_1 is expressed in minutes:

$$log_{10}\big(e_0(T_1)\big) = -0.5923 \cdot log_{10} T_1 - 1.4163 \tag{31}$$

$$log_{10}\big(P_0(T_1)\big) = -0.8789 \cdot log_{10} T_1 + 0.7363 \tag{32}$$

For each TBR at each time step, for each accumulation T_1, the nugget can be calculated as:

$$c_{0_i}(t, T_1) = \sigma_{err}(T_1, P_T)^2 = \left(e_0(T_1) + \frac{P_0(T_1)}{P_T}\right)^2 \tag{33}$$

Besides TBRs, there are other types of rain gauges commonly used. For example, the Royal Meteorological Institute of the Netherlands (KNMI) uses a network of 33 highly accurate automatic rain gauges that measure the water level using the accurate measurement of a floating device position on the water surface. This type of rain gauges is more precise than the TBR type, especially at low rainfall intensity, it is subject to less measuring errors, and it is calibrated by the KNMI (Brandsma, 2014; Wauben, 2006). The KNMI automatic rain gauges are highly accurate devices, but only 33 are available to cover the whole Netherlands. To improve the spatial coverage, the KNMI also collects the data from a much denser network of 325 manual rain gauges. The manual rain gauges are neither TBR nor floating-device rain gauges, and do not recording data automatically: volunteers read the water level every day at 08:00 CET and communicate the reading to the KNMI that collects the set of daily accumulations. The German Meteorological Service (Deutscher Wetterdienst – DWD) instead has a network of around 1100 automatic rain gauges using a weighting system (Winterrath et al., 2012). Information on the accuracy and uncertainty associated to the measurements from different types of rain gauges can often be found in reports from the meteorological services (Brandsma, 2014; Wauben, 2006; Winterrath et al., 2012).

6 Integration of radar uncertainty in radar-gauge merged rainfall

As discussed in Section 2, radar QPE are subject to a multitude of errors, the majority of which are non-stationary in space and are caused by space-variant factors. The use of fixed *Z-R* relationships does not take into account the dependency of the relationships on the Drop Size Distribution (DSD), (Doviak, 1983; Marshall et al., 1947) or the presence of solid precipitation (Marshall and Gunn, 1952; Smith, 1984), which spatially and temporally vary with atmospheric conditions, but also with radar beam elevation. Radar beams can interfere with the terrain surface, resulting in partial or total beam blockage (Joss and Lee, 1995; Krajewski et al., 2006; Lang et al., 2009) or clutter (Hubbert et al., 2009a, 2009b; Islam et al., 2012c; Rico-Ramirez and Cluckie, 2008). Variable atmospheric conditions can influence the signal propagation as well, resulting in anomalous propagation (Grecu and Krajewski, 2000; Moszkowicz et al., 1994; Pamment and Conway, 1998; Rico-Ramirez and Cluckie, 2008; Steiner and Smith, 2002) or attenuation (Atlas and Banks, 1951; Delrieu et al., 2000; Meneghini, 1978; Uijlenhoet and Berne, 2008). The vertical variability of the atmospheric conditions and reflectivity affects the rainfall estimation differently along the propagation range (Andrieu et al., 1995; Andrieu and Creutin, 1995; Kirstetter et al., 2013; Krajewski et al., 2011; Qi et al., 2013; Vignal et al., 1999), especially when the radar beam intersects the layer where solid precipitation melts into liquid precipitation, which is characterised by high-reflectivity that affects the measurements, called “bright band” (Austin and Bernis, 1950; Hall et al., 2015; Rico-Ramirez et al., 2005; Rico-Ramirez and Cluckie, 2007; Smith, 1986; Zhang and Qi, 2010). The estimation of precipitation is subject to additional errors increasing with the range, due for example to beam broadening, beam elevation increase, and earth curvature effects (Ge et al., 2010; Kitchen and Jackson, 1993; Ryzhkov, 2007). National meteorological services usually apply corrections for these errors (Harrison et al., 2012; Joss et al., 1997; Wessels, 2006), especially when technologies like doppler capabilities or dual polarization are available (Bringi and Chandrasekar, 2004; Doviak and Zrnic, 1993), but a residual uncertainty is unavoidable.

Although KED merging helps improving the accuracy of the rainfall estimates, merged rainfall products are still subject to errors, which are spatially variable. The KED merging approach offers a starting point for radar rainfall uncertainty estimation through the kriging variance. However, the kriging variance is an estimation of the uncertainty due to interpolation, spatial variability of the process mean, in this case represented by a regression of the radar rainfall, or expected measurement uncertainty, as illustrated in the previous section. The variability of rainfall uncertainty due to external factors (like terrain elevation or distance from the radar) affecting radar QPEs uncertainty are not taken into consideration. Radar QPEs are used as a trend in KED and the spatial variability of radar residual errors affects merged rainfall estimates.

A method to include radar uncertainty spatial variability in a KED merging approach is here presented. KED with Non-Stationary Variance (KED-NSV), based on the formulation of Lark, (2009), has been adapted to hydrology by Wadoux et al., (2017). The idea is to modify the standard KED algorithm in order to relax the assumption of stationary process variance, and to model the process standard deviation as a linear function of external covariates, similarly to how the mean is modelled in the regular KED formulation. This allows us to consider factors that affect the spatial variability of the radar QPE, and to modify the spatial variability of the merged rainfall uncertainty accordingly.

6.1 Methods

6.1.1 Kriging with External Drift and Non-Stationary Variance (KED-NSV)

The model, as proposed by Lark, (2009) and applied to hydrology by Wadoux et al., (2017), extends the formulation of KED (Equation 17) to consider the process residual variance non-stationary as well, following a modelling approach similar to the one used for the process mean. The studied field $P(x)$ is therefore modelled as:

$$P(x) = m(x) + \sigma(x)\epsilon(x) \tag{34}$$

where $\sigma(x)$ is the spatial standard deviation, and $\epsilon(x)$ is a zero-mean, unit variance, normally distributed and spatially correlated standardised residual field. Similarly to the mean (Equation 18), the spatial standard deviation is modelled as a linear function of covariates:

$$\sigma(x) = \sum_{l=0}^{L} \beta_l \cdot q_l(x) \tag{35}$$

where $q_l(x)$ are L covariates at location x, β_l are regression coefficients, and we assume $q_0(x) = 1$, so that β_0 is an intercept. Considering the observations $G(x_i)$ at locations $x_i, i = 1,2,\dots,n$, and organising the measurements in a vector $\boldsymbol{G}$, Equation 34 can be written in matricial form:

$$\boldsymbol{G} = \boldsymbol{F\alpha} + \boldsymbol{H\epsilon} \tag{36}$$

where $\boldsymbol{F}$ and $\boldsymbol{\alpha}$ are respectively the matrix of $n \times (K+1)$ covariates $f_k(x)$ and the vector of linear regression coefficients α_k at n locations from Equation 17, $\boldsymbol{\epsilon}$ is the vector of n standardised residuals with correlation matrix $\boldsymbol{\rho}$, and $\boldsymbol{H}$ is an $n \times n$ diagonal matrix:

$$\boldsymbol{H} = diag\{\boldsymbol{Q} \cdot \boldsymbol{\beta}\} \tag{37}$$

where $\boldsymbol{Q}$ is the $n \times (L+1)$ matrix of standard deviation covariates at n locations, while $\boldsymbol{\beta}$ is a $(L+1)$ vector of regression coefficients for the standard deviation, from Equation 35. To define the correlation matrix $\boldsymbol{\rho}$, we apply an isotropic exponential correlogram $\rho(d)$ to the distance between the measurements:

$$\rho(d) = \begin{cases} 1 & d = 0 \\ \rho_0 \left\{ \exp\left(-\frac{d}{h}\right) \right\} & d > 0 \end{cases} \tag{38}$$

where d is the Euclidean distance between two measurements, ρ_0 is the micro-scale correlation parameter, equal to one minus the nugget-to-sill ratio, and h is the range parameter. From now on, KED will be treated as a special case of KED-NSV, where the only considered covariate is $q_0(x) = 1$, thus $\sigma(x) = \beta_0$.

6.1.2 Parameter prediction and variance estimation

There are two sets of parameters to estimates: the regression coefficients for the mean, $\boldsymbol{\alpha}$, and the parameters of the stochastic part of Equation 36, $\Phi = [\boldsymbol{\beta}, \rho_o, h]$. The use of Maximum Likelihood estimation would allow estimation of all model parameters, but would also make the estimation of the standard deviation parameters depend too much on the trend parameters. Therefore, here the estimation of $\boldsymbol{\alpha}$, which is more straightforward, is done with a Generalised Least Square (GLS) approach, while for Φ a Restricted Maximum Likelihood (REML) approach is used (Patterson and Thompson, 1971). The derivation is not reported here and can be found in Wadoux et al., (2017). To minimise the negative log-likelihood function, a shuffled complex evolution method, developed at the University of Arizona (SCE-UA) (Duan et al., 1994, 1992) can be used. Obtaining $\widehat{\boldsymbol{\alpha}}, \widehat{\boldsymbol{\beta}}, \widehat{\rho_0}$ and $\hat{h}$, both the kriging prediction and variance can be estimated.

The kriging prediction in a new location x_0 is derived from Equation 34:

$$\hat{P}(x_0) = \boldsymbol{f_0}'\widehat{\boldsymbol{\alpha}} + \boldsymbol{q_0}\widehat{\boldsymbol{\beta}}\hat{\boldsymbol{\epsilon}}(x_0) \tag{39}$$

where $\boldsymbol{f_0}$ and $\boldsymbol{q_0}$ are the trend and variance covariates respectively, as observed at estimation location x_0. $\hat{\boldsymbol{\epsilon}}(x_0)$ are the kriged standardised residuals. The kriging variance instead is estimated as follows (Cressie, 1993):

$$\sigma^2(x_0) = \boldsymbol{q_0}\widehat{\boldsymbol{\beta}} - \boldsymbol{c_0'C^{-1}c_0} + (\boldsymbol{f_0} - \boldsymbol{F'C^{-1}c_0})'(\boldsymbol{F'C^{-1}C})^{-1}(\boldsymbol{f_0} - \boldsymbol{F'C^{-1}c_0}) \tag{40}$$

where $\boldsymbol{C} = \boldsymbol{H\rho H'}$, is the covariance matrix between measurement points, while $\boldsymbol{c_0}$ is a vector of covariances between the measurements points and the observation location.

6.1.3 Covariate selection

The radar QPE is generally the only considered covariate for the mean. As concerns which covariates can be meaningful in explaining the spatial non-stationarity of the kriging variance and how many to use, in order to optimise the model, different combination of external covariates can be tested. Three different covariates are considered by Wadoux et al., (2017):

a) a map of the distance to the closest radar;
b) the SRTM digital elevation model (DEM);
c) a radar beam blockage map derived by the DEM (Rico-Ramirez et al., 2009);

Cecinati et al., (2017), consider the same study area, but do not use the blockage map. They introduce instead the following external factors:

d) a static clutter map, obtained from the DEM as in (Rico-Ramirez et al., 2009);
e) a mean residual map, obtained kriging the average of residuals between rain gauges and radar over time;
f) the radar rainfall estimate corresponding to the studied time step.

While the radar rainfall estimate is time-variant, the other covariates are stationary in time. All covariates are scaled to have values between 0 and 1, to be comparable in terms of absolute value. The covariates are represented in Figure 6.1.

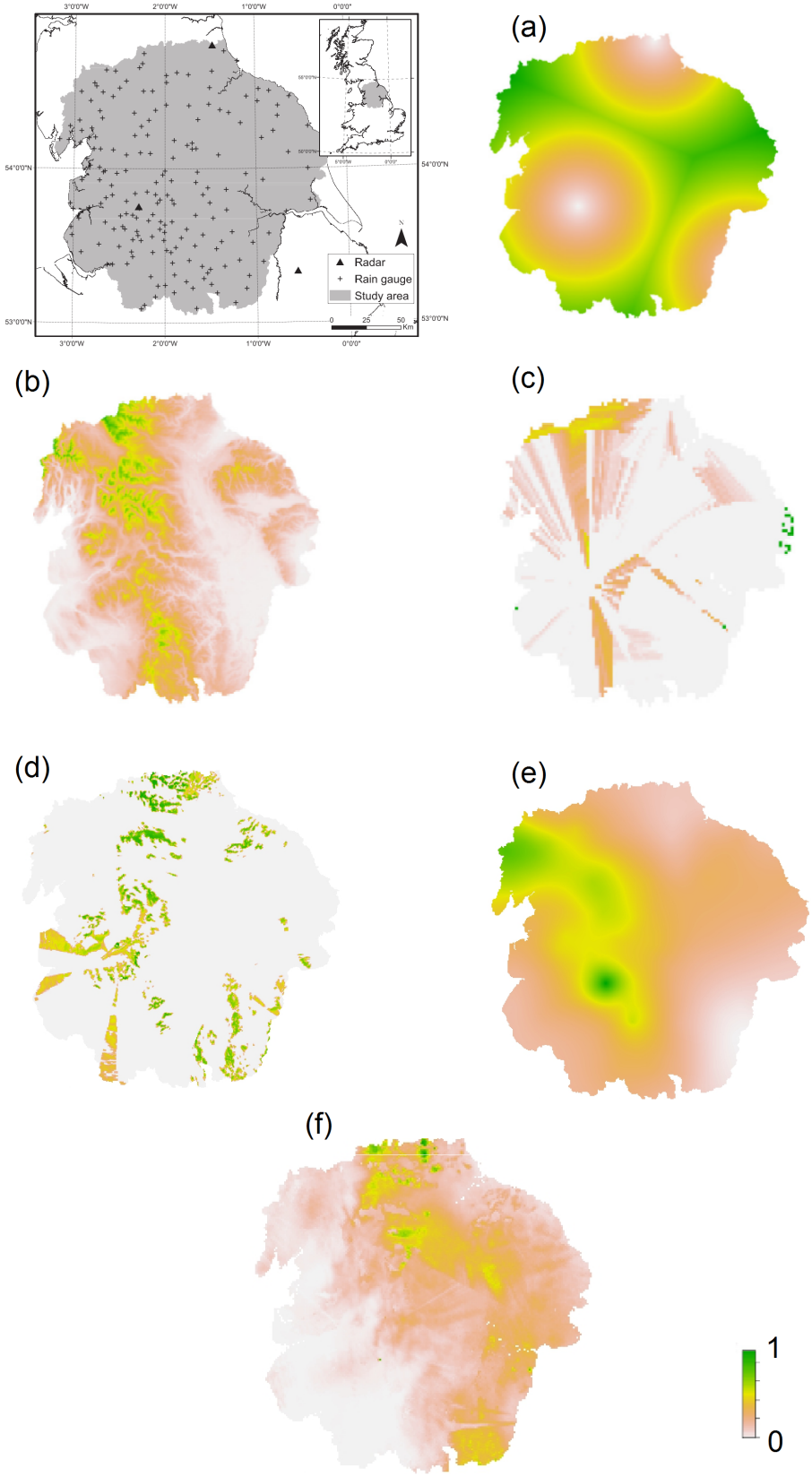

Figure 6.1 - Study area used in Wadoux et al., (2017) *and* Cecinati et al., (2017)*, which is a large portion of Northern England, together with the used covariates, numbered according to the list in Section 6.1.3*

7 Ensembles using kriging rainfall uncertainty

Rainfall is one of the main inputs in a variety of models: hydrological, water quality, urban drainage, water resources, ecological, agricultural, and more. The propagation of the rainfall uncertainty in a model is a key element to evaluate how sensitive a model is to the input uncertainty. Analytical propagation methods are rarely applicable, both because many models have a complex structure, and because rainfall has a multivariate distribution with statistical characteristics varying in space and time. The most popular and effective technique to evaluate rainfall input uncertainty propagation is to use an ensemble approach. Similarly to other Monte Carlo techniques, the idea underlying the use of ensembles is that we can sample the probability distribution of rainfall in order to generate a large number of possible alternative model inputs, use them one by one in the analysed model, and observe the distribution of the model outputs. As mentioned, rainfall has a multivariate distribution and its sampling and ensemble generation requires to respect the spatial and temporal characteristics of the process.

Section 3 presented a methodology to generate ensembles of radar QPE and deriving the uncertainty estimation using rain gauges as a reference, while neglecting rain gauge uncertainty. Here, a method to generate rainfall ensembles from a kriging product, which can include a comprehensive uncertainty estimation, is presented.

The model considers each ensemble member as the sum of a mean, equal for all ensemble members, and a variable error component. The mean is modelled as the kriging mean. The error components are derived from the kriging variance.

Each ensemble member is modelled as:

$$\hat{P}_i(x,t) = P_{KED}(x,t) + \sigma_{KED}(x,t) \cdot \epsilon_i(x,t) \tag{41}$$

where $\hat{P}_i(x,t)$ is the i^{th} ensemble member; $P_{KED}(x,t)$ and $\sigma_{KED}(x,t)$ are, respectively, the KED mean and the KED standard deviation; and $\epsilon_i(x,t)$ is a standardized, zero-mean, spatially auto-correlated residual field.

To generate $\epsilon_i(x,t)$, an unconditional simulation is used, with mean equal to zero, and standard deviation equal to one, using the residuals' variogram at the corresponding time step. Subsequently, to reconstruct the auto-correlation of the residuals, a $AR(2)$ model is used. The auto-correlation and the parameters of the $AR(2)$ model are derived from the residuals time series (Germann et al., 2009).

A large number of such fields can be generated with unconditional simulations, respecting the spatial characteristics of the observed rainfall (Sawicka and Heuvelink, 2016a, 2016b). Once a large number of possible alternative rainfall time series are generated, they can be used as model input, obtaining a large number of outputs. The obtained outputs can be used to reconstruct the output probability distribution, and therefore evaluate the uncertainty in the output due to the input uncertainty.

8 Summary

This deliverable presented a set of geo-statistical tools that can be used to study, characterise and propagate the uncertainty in radar QPE and in merged radar-gauge rainfall estimates. Each section described a different tool.

In **Section 2**, a logarithmic error model for radar QPE uncertainty was introduced. The model considers radar QPE random errors additive in the logarithmic domain, thus multiplicative in the original domain. The model, consistent with previous literature, has the advantage of producing Gaussian residual errors. This model feature makes it easier to: 1) characterise the errors with only a mean, a variance and a variogram; 2) produce synthetic error with the same characteristics of the observed errors that can be used for ensemble applications, as presented in Section 3.

In **Section 3**, an innovative method to generate radar QPE ensembles was presented as a tool to model and propagate radar rainfall uncertainty. Compared to other methods based on the use of the residual error covariance matrix, the presented method introduces some advantages. Firstly, the use of variograms allows for a faster and more flexible calculation of spatial correlation of errors, at the point that a time-variant error characterisation is possible. The time-variant application allows us to capture temporary phenomena that may affect the nature of errors, generating ensembles that are specific for the simulated time step. The adoption of a logarithmic multiplicative error model allows for Gaussian modelling of the errors that makes the error characterisation and the alternative error field generation easier. As a drawback, it introduces some bias in the back-transformation. In this application, the problem of mean and variance inflation is addressed with a linear re-adjustment that corrects the absolute values of the ensemble members without affecting their spatial characteristics. Using the overall mean and standard deviation of the ensemble for adjustment, the adjusting method forces the whole ensemble to have the observed statistical characteristics, but does not coerce the single ensemble members. Another significant advantage of the presented method is that using conditional simulations allows us to generate spatially-correlated Gaussian realisations of the random fields. Therefore, no interpolation of the simulated error components is needed. The use of interpolation has a smoothing effect due to the use of the kriging mean, rather than the full probabilistic kriging outcome. This can partially cover the problem of mean and variance inflation, but also modifies the spatial characteristics of the errors. The errors are generated with conditional simulations, where sufficient error observations were available, drawing correlated realisation for the conditional distribution of the whole grid. Conditioning the simulation to the observations allows us to partially reproduce the spatial variability of the error statistical properties that is neglected using an omni-directional variogram.

In **Section 4**, Kriging with External Drift (KED) was introduced. KED is a very popular merging method, thanks to its good performance, its robustness and its limited computational requirements. Being a kriging method, KED is based on the concept of minimising the variance between the estimation and the true process. Thanks to its probabilistic nature, KED offers a good platform for uncertainty analysis, thanks to the possibility to calculate the kriging variance. The kriging variance is the variance associated to the rainfall estimation after minimisation, and includes the uncertainty due to interpolation and process observed decorrelation. The decorrelation of the modelled process in space is estimated through a variogram. Two methodologies to calculate the variogram for KED are presented, taking into consideration that the KED variogram is estimated on rainfall residuals (difference between the process and its estimated mean) and that the presence of a large number

of zero values can make the number of rain gauge observations too small for a correct, time-variant estimation of the variogram. For this reason, the two suggested methods propose to use the radar for the variogram estimation, using a subset of the wet pixels, or a Fast Fourier Transform approach, respectively.

In **Section 5**, the uncertainty associated to rain gauge measurements was considered. Although rain gauges are known to be affected by a multitude of errors, often dependent on the rainfall intensity, rarely the measurement uncertainty is considered in merged radar-rain gauge rainfall products. When uncertainty is considered, it is often approximated with a stationary model, invariant in space and time, and independent from the rainfall intensity. Section 5 presents Kriging for Uncertain Data (KUD to include measurement uncertainty in the overall uncertainty estimation of kriging rainfall products. The uncertainty for each rain gauge can be modelled separately as a function of the rain gauge type, of the accumulation interval, and of the rainfall intensity, therefore it is neither stationary in space nor in time. The overall rainfall uncertainty is estimated using the kriging variance.

Section 6 introduced a merging technique named Kriging with External Drift and Non-Stationary Variance. The technique is able to consider the non-stationarity of the process variance, and extends the KED formulation to consider the process standard deviation as a linear function of external factors affecting the rainfall uncertainty. In particular, factors influencing the radar QPE uncertainty are considered.

Finally, in **Section 7**, a technique to generate ensembles from kriging products, including a kriging prediction and a kriging variance, was presented. The algorithm allows to propagate the uncertainty associated to merged radar-gauge rainfall products into different types of models, taking into consideration the spatial and temporal correlation of rainfall uncertainty.

The methodologies presented in this deliverable are modular, and can be applied or easily adapted to KED and other kriging-based merging methods. The methodologies (KUD, KED-NSV, Gaussian transformations, downscaling techniques, ensembles, etc.) were presented one by one, but, in practice, they can easily be combined to consider several aspects of uncertainty at the same time. However, it must be kept in mind that a trade-off between model complexity, necessary assumptions and model identifiability is often necessary. Indeed, a more complex and descriptive model is not always a better model, in terms of result accuracy, due to the necessity of making additional assumptions, or to the increasing difficulty in identifying the model parameters. In practice, each case study should be evaluated independently to understand what the main causes of uncertainty are, and what aspects are more important to address. This deliverable offers a wide selection of tools that can help to model and address rainfall uncertainty. We hope that these tools can be used not only by researchers, but also by practitioners in order to analyse how rainfall uncertainty propagates through natural and urban hydrological models.

References

AghaKouchak, A., Bárdossy, A., Habib, E., 2010. Copula-based uncertainty modelling: Application to multisensor precipitation estimates. Hydrol. Process. 24, 2111–2124. doi:10.1002/hyp.7632

AghaKouchak, A., Habib, E., Bárdossy, A., 2010. Modeling Radar Rainfall Estimation Uncertainties: Random Error Model. J. Hydrol. Eng. 15, 265–274. doi:10.1061/(ASCE)HE.1943-5584.0000185

Anagnostou, E., Krajewski, W.F., 1999. Uncertainty Quantification of Mean-Areal Radar-Rainfall Estimates. J. Atmos. Ocean. Technol. 206–215.

Andrieu, H., Creutin, J.D., 1995. Identification of Vertical Profiles of Radar Reflectivity for Hydrological Applications Using an Inverse Method. Part I: Formulation. J. Appl. Meteorol. doi:10.1175/1520-0450(1995)034<0225:IOVPOR>2.0.CO;2

Andrieu, H., Delrieu, G., Creutin, J., 1995. Identification of Vertical Profiles of Radar Reflectivity For Hydrological Applications Using on Inverse Method . Part 2: Sensitivity Analysis And Case-Study. J. Appl. Meteorol. doi:10.1175/1520-0450(1995)0342.0.CO;2

Atlas, D., Banks, H.C., 1951. The Interpretation of Microwave Reflections From Rainfall. J. Meteorol. 8, 271–282. doi:10.1175/1520-0469(1951)008<0271:tiomrf>2.0.co;2

Austin, P.M., 1987. Relation between Measured Radar Reflectivity and Surface Rainfall. Mon. Weather Rev. 115, 1053–1070. doi:10.1175/1520-0493(1987)115<1053:RBMRRA>2.0.CO;2

Austin, P.M., Bernis, A.C., 1950. A quantitative study of the “bright band” in radar precipitation echoes. J. Meteorol. 7, 145–151. doi:10.1175/1520-0469(1950)007<0145:AQSOTB>2.0.CO;2

Berndt, C., Rabiei, E., Haberlandt, U., 2014. Geostatistical merging of rain gauge and radar data for high temporal resolutions and various station density scenarios. J. Hydrol. 508, 88–101. doi:10.1016/j.jhydrol.2013.10.028

Berne, A., Delrieu, G., Creutin, J., Obled, C., 2004. Temporal and spatial resolution of rainfall measurements required for urban hydrology. J. Hydrol. 299, 166–179. doi:10.1016/j.jhydrol.2004.08.002

Berne, A., Krajewski, W.F., 2013. Radar for hydrology: Unfulfilled promise or unrecognized potential? Adv. Water Resour. 51, 357–366. doi:10.1016/j.advwatres.2012.05.005

Brandsma, T., 2014. Comparison of automatic and manual precipitation networks in the Netherlands. De Bilt.

Bringi, V.N., Chandrasekar, V., 2004. Polarimetric Doppler Weather Radar. Cambridge Universtiy Press, Cambridge.

Bringi, V.N., Keenan, T.D., Chandrasekar, V., 2001. Correcting C-band radar reflectivity and differential reflectivity data for rain attenuation: A self-consistent method with constraints. IEEE Trans. Geosci. Remote Sens. 39, 1906–1915. doi:10.1109/36.951081

Bringi, V.N., Rico-Ramirez, M. a., Thurai, M., 2011. Rainfall Estimation with an Operational Polarimetric C-Band Radar in the United Kingdom: Comparison with a Gauge Network and Error Analysis. J. Hydrometeorol. 12, 935–954. doi:10.1175/JHM-D-10-05013.1

Cecinati, F., Wadoux, A., Rico-Ramirez, M.A., Heuvelink, G.B.M., 2017. Rainfall estimation using a non-stationary geostatistical model and uncertain measurements, in: 2017 International Symposium Weather Radar and Hydrology. Seoul.

Chiles, J.-P., Delfiner, P., 1999. Geostatistics: Modeling Spatial Uncertainty. Wiley Ser. Probab. Stat. Appl. Probab. Stat. Sect. xi, 695. doi:10.1007/s11004-012-9429-y

Ciach, G.J., 2003. Local Random Errors in Tipping-Bucket Rain Gauge Measurements. J. Atmos.

Ocean. Technol. 20, 752–759.

Ciach, G.J., Krajewski, W.F., Villarini, G., 2007. Product-Error-Driven Uncertainty Model for Probabilistic Quantitative Precipitation Estimation with NEXRAD Data. J. Hydrometeorol. 8, 1325–1347. doi:10.1175/2007JHM814.1

Clark, I., 2010. Statistics or geostatistics? Sampling error or nugget effect? J. South. African Inst. Min. Metall. 110, 307–312.

Cluckie, I.A.N.D., Rico-Ramirez, M.A., 2004. Weather radar technology and future developments 11–20.

Cressie, N., 1990. The origins of kriging. Math. Geol. 22, 239–252. doi:10.1007/BF00889887

Cressie, N., 1985. Fitting variogram models by weighted least squares. J. Int. Assoc. Math. Geol. 17, 563–586. doi:10.1007/BF01032109

Cressie, N.A.C., 1993. Statistics for Spatial Data.

Creutin, J.D., Delrieu, G., Lebel, T., 1988. Rain Measurement by Raingage-Radar Combination: A Geostatistical Approach. J. Atmos. Ocean. Technol. doi:10.1175/1520-0426(1988)005<0102:RMBRRC>2.0.CO;2

Dai, Q., Han, D., Rico-Ramirez, M., Srivastava, P.K., 2014a. Multivariate distributed ensemble generator: A new scheme for ensemble radar precipitation estimation over temperate maritime climate. J. Hydrol. 511, 17–27. doi:10.1016/j.jhydrol.2014.01.016

Dai, Q., Rico-Ramirez, M. a., Han, D., Islam, T., Liguori, S., 2014b. Probabilistic radar rainfall nowcasts using empirical and theoretical uncertainty models. Hydrol. Process. n/a-n/a. doi:10.1002/hyp.10133

De Marsily, G., 1986. Quantitative Hydrogeology.

Delhomme, J.P., 1979. Spatial Variability and Uncertainty in Groundwater Flow Parameters - A Geostatitical Approach. Water Resour. Res. 15, 269–280.

Delrieu, G., Andrieu, H., Creutin, J.D., 2000. Quantification of Path-Integrated Attenuation for X- and C-Band Weather Radar Systems Operating in Mediterranean Heavy Rainfall. J. Appl. Meteorol. 39, 840–850. doi:10.1175/1520-0450(2000)039<0840:QOPIAF>2.0.CO;2

Delrieu, G., Wijbrans, A., Boudevillain, B., Faure, D., Bonnifait, L., Kirstetter, P.E., 2014. Geostatistical radar-raingauge merging: A novel method for the quantification of rain estimation accuracy. Adv. Water Resour. 71, 110–124. doi:10.1016/j.advwatres.2014.06.005

Doviak, R.J., 1983. A Survey of Radar Rain Measurement Techniques. J. Clim. Appl. Meteorol. doi:10.1175/1520-0450(1983)022<0832:ASORRM>2.0.CO;2

Doviak, R.J., Zrnic, D.S., 1993. Doppler Radar and Weather Observations, Second Edi. ed. Academic Press, Inc.

Duan, Q., Sorooshian, S., Gupta, V.K., 1994. Optimal use of the SCE-UA global optimization method for calibrating watershed models. J. Hydrol. 158, 265–284. doi:10.1016/0022-1694(94)90057-4

Duan, Q., Sorooshian, S., Gupta, H. V., Gupta, V., 1992. Effective and efficient global optimization for conceptual rainfall-runoff models. Water Resour. Res. 28, 1015–1031. doi:10.1029/91WR02985

Einfalt, T., Arnbjerg-nielsen, K., Golz, C., Jensen, N., Quirmbach, M., Vaes, G., Vieux, B., 2004. Towards a roadmap for use of radar rainfall data in urban drainage. J. Hydrol. 299, 186–202. doi:10.1016/j.jhydrol.2004.08.004

Erdin, R., Frei, C., Künsch, H.R., 2012. Data Transformation and Uncertainty in Geostatistical

Combination of Radar and Rain Gauges. J. Hydrometeorol. 13, 1332–1346. doi:10.1175/JHM-D-11-096.1

Fabry, F., 2015. Radar Meteorology - Principles and Practice. Cambridge University Press, Cambridge.

Fabry, F., Bellon, A., Duncan, M.R., Austin, G.L., 1994. High resolution rainfall measurements by radar for very small basins: the sampling problem reexamined. J. Hydrol. 161, 415–428. doi:10.1016/0022-1694(94)90138-4

Fabry, F., Zawadzki, I., 1995. Long-Term Radar Observations of the Melting Layer of Precipitation and Their Interpretation. J. Atmos. Sci. 52, 838–851. doi:10.1175/1520-0469(1995)052<0838:LTROOT>2.0.CO;2

Friedrich, K., Germann, U., Gourley, J.J., Tabary, P., 2007. Effects or radar beam shielding on rainfall estimation for the polarimetric C-band radar. J. Atmos. Ocean. Technol. 24, 1839–1859. doi:10.1175/JTECH2085.1

Gabriele, S., Chiaravalloti, F., Procopio, A., 2017. Radar-rain-gauge rainfall estimation for hydrological applications in small catchments. Adv. Geosci. 44, 61–66. doi:10.5194/adgeo-44-61-2017

Ge, G., Gao, J., Brewster, K., Xue, M., 2010. Impacts of Beam Broadening and Earth Curvature on Storm-Scale 3D Variational Data Assimilation of Radial Velocity with Two Doppler Radars. J. Atmos. Ocean. Technol. 27, 617–636. doi:10.1175/2009jtecha1359.1

Germann, U., Berenguer, M., Sempere-Torres, D., Zappa, M., 2009. REAL – Ensemble radar precipitation estimation for hydrology in mountainous region. Q. J. R. Meteorol. Soc 135, 445–456. doi:10.1002/qj.375

Gonzalez-Ramirez, E., Rico-Ramirez, M.A., Cluckie, I., Vargas, J.I.D.L.R., Alaniz-Lumbreras, D., 2011. Design of a clutter modelling algorithm based on SRTM DEM Data and adaptive signal processing methods . 1–6.

Goudenhoofdt, E., Delobbe, L., 2009. Evaluation of radar-gauge merging methods for quantitative precipitation estimates. Hydrol. Earth Syst. Sci. Discuss. 5, 2975–3003. doi:10.5194/hessd-5-2975-2008

Grecu, M., Krajewski, W.F., 2000. An efficient methodology for detection of anomalous propagation echoes in radar reflectivity data using neural networks. J. Atmos. Ocean. Technol. 17, 121–129. doi:10.1175/1520-0426(2000)017<0121:AEMFDO>2.0.CO;2

Grimes, D.I.F., Pardo-Iguzquiza, E., Bonifacio, R., 1999. Optimal areal rainfall estimation using raingauges and satellite data [WWW Document]. J. Hydrol. URL http://ac.els-cdn.com/S002216949900092X/1-s2.0-S002216949900092X-main.pdf?_tid=d7d69ca6-6b5c-11e5-8327-00000aacb35e&acdnat=1444048400_66b46ff51d3e96b48e67d42765c2acfe (accessed 10.5.15).

Haberlandt, U., 2007. Geostatistical interpolation of hourly precipitation from rain gauges and radar for a large-scale extreme rainfall event. J. Hydrol. 332, 144–157. doi:10.1016/j.jhydrol.2006.06.028

Habib, E., Ciach, G.J., Krajewski, W.F., 2004. A method for filtering out raingauge representativeness errors from the verification distributions of radar and raingauge rainfall. Adv. Water Resour. 27, 967–980. doi:10.1016/j.advwatres.2004.08.003

Habib, E., Krajewski, W.F., Kruger, A., 2001. Sampling Errors of Tipping-Bucket Rain Gauge Measurements. J. Hydrol. Eng. 6, 159–166. doi:10.1061/(ASCE)1084-0699(2001)6:2(159)

Habib, E.H., Meselhe, E. a., Aduvala, A. V., 2008. Effect of Local Errors of Tipping-Bucket Rain Gauges on Rainfall-Runoff Simulations. J. Hydrol. Eng. 13, 488–496. doi:10.1061/(ASCE)1084-

0699(2008)13:6(488)

Hall, W., Rico-Ramirez, M.A., Krämer, S., 2015. Classification and correction of the bright band using an operational C-band polarimetric radar. J. Hydrol. 531, 248–258. doi:10.1016/j.jhydrol.2015.06.011

Harrison, D.L., Driscoll, S.J., Kitchen, M., 2000. Improving precipitation estimates from weather radar using quality control and correction techniques. Meteorol. Appl. 7, 135–144. doi:10.1017/S1350482700001468

Harrison, D.L., Norman, K., Pierce, C., Gaussiat, N., 2012. Radar products for hydrological applications in the UK. Proc. Inst. Civ. Eng. - Water Manag. 165, 89–103. doi:10.1680/wama.2012.165.2.89

Hasan, M.M., Sharma, A., Johnson, F., Mariethoz, G., Seed, A., 2014. Correcting bias in radar Z–R relationships due to uncertainty in point rain gauge networks. J. Hydrol. 519, 1668–1676. doi:10.1016/j.jhydrol.2014.09.060

Hubbert, J.C., Dixon, M., Ellis, S.M., 2009a. Weather Radar Ground Clutter. Part II: Real-Time Identification and Filtering. J. Atmos. Ocean. Technol. 26, 1181–1197. doi:10.1175/2009JTECHA1160.1

Hubbert, J.C., Dixon, M., Ellis, S.M., Meymaris, G., 2009b. Weather radar ground clutter. Part I: Identification, modeling, and simulation. J. Atmos. Ocean. Technol. 26, 1165–1180. doi:10.1175/2009JTECHA1159.1

Hyvärinen, A., Oja, E., 2000. Independent Component Analysis : Algorithms and Applications. Neural Networks 13, 411–430.

Islam, T., Rico-Ramirez, M.A., Han, D., 2012a. Tree-based genetic programming approach to infer microphysical parameters of the DSDs from the polarization diversity measurements. Comput. Geosci. 48, 20–30. doi:10.1016/j.cageo.2012.05.028

Islam, T., Rico-Ramirez, M.A., Han, D., Bray, M., Srivastava, P.K., 2012b. Fuzzy logic based melting layer recognition from 3 GHz dual polarization radar: appraisal with NWP model and radio sounding observations. Theor. Appl. Climatol. 112, 317–338. doi:10.1007/s00704-012-0721-z

Islam, T., Rico-Ramirez, M.A., Han, D., Srivastava, P.K., 2012c. Artificial intelligence techniques for clutter identification with polarimetric radar signatures. Atmos. Res. 109–110, 95–113. doi:10.1016/j.atmosres.2012.02.007

Jewell, S.A., Gaussiat, N., 2015. An assessment of kriging-based rain-gauge-radar merging techniques. Q. J. R. Meteorol. Soc. 141, 2300–2313. doi:10.1002/qj.2522

Joanes, D.N., Gill, C.A., 1998. Comparing measures of sample skewness and kurtosis. J. R. Stat. Soc. Ser. D (The Stat. 47, 183–189. doi:10.1111/1467-9884.00122

Joss, J., Lee, R., 1995. The Application of Radar-Gauge Comparisons to Operational Precipitation Profile Corrections. J. Appl. Meteorol. 34, 2612–2630. doi:10.1175/1520-0450(1995)034<2612:TAORCT>2.0.CO;2

Joss, J., Schädler, B., Galli, G., Cavalli, R., Boscacci, M., Held, E., Della Bruna, G., Kappenberger, G., Nespor, V., Spiess, R., 1997. Operational use of radar for precipitation measurements in Switzerland. Locarno.

Kirstetter, P.E., Andrieu, H., Boudevillain, B., Delrieu, G., 2013. A Physically based identification of vertical profiles of reflectivity from volume scan radar data. J. Appl. Meteorol. Climatol. 52, 1645–1663. doi:10.1175/JAMC-D-12-0228.1

Kirstetter, P.-E., Delrieu, G., Boudevillain, B., Obled, C., 2010. Toward an error model for radar quantitative precipitation estimation in the Cévennes–Vivarais region, France. J. Hydrol. 394,

28–41. doi:10.1016/j.jhydrol.2010.01.009

Kirstetter, P.-E., Gourley, J.J., Hong, Y., Zhang, J., Moazamigoodarzi, S., Langston, C., Arthur, A., 2015. Probabilistic precipitation rate estimates with ground-based radar networks 1–56.

Kitchen, M., Brown, R., Davies, A.G., 1994. Real-Time Correction of Weather Radar Data for the Effects of Bright Band, Range and Orographic Growth in Widespread Precipitation. Q. J. R. Meteorol. Soc. 120, 1231–1254.

Kitchen, M., Jackson, P.M., 1993. Weather radar performance at long range - simulated and observed. J. Appl. Meteorol. 32, 975–985.

Krajewski, W.F., 1987. Cokriging radar-rainfall and rain gage data. J. Geophys. Res. 92, 9571. doi:10.1029/JD092iD08p09571

Krajewski, W.F., Ntelekos, A.A., Goska, R., 2006. A GIS-based methodology for the assessment of weather radar beam blockage in mountainous regions: Two examples from the US NEXRAD network. Comput. Geosci. 32, 283–302. doi:10.1016/j.cageo.2005.06.024

Krajewski, W.F., Vignal, B., Seo, B.-C., Villarini, G., 2011. Statistical model of the range-dependent error in radar-rainfall estimates due to the vertical profile of reflectivity. J. Hydrol. 402, 306–316. doi:10.1016/j.jhydrol.2011.03.024

Krige, D.G., 1952. A Statistical Approach to Some Basic Mine Valuation Problems on the Witwatersrand. J. Chem. Metall. Min. Soc. South Africa. doi:10.2307/3006914

Lang, T.J., Nesbitt, S.W., Carey, L.D., 2009. On the correction of partial beam blockage in polarimetric radar data. J. Atmos. Ocean. Technol. 26, 943–957. doi:10.1175/2008JTECHA1133.1

Lark, R.M., 2009. Kriging a soil variable with a simple nonstationary variance model. J. Agric. Biol. Environ. Stat. 14, 301–321. doi:10.1198/jabes.2009.07060

Le Ravalec, M., Noetinger, B., Hu, L.Y., 2000. The FFT moving average (FFT-MA) generator: An efficient numerical method for generating and conditioning Gaussian simulations. Math. Geol. 32, 701–723. doi:10.1023/A:1007542406333

Lebel, T., Bastin, G., Obled, C., Creutin, J.D., 1987. On the accuracy of areal rainfall estimation: A case study. Water Resour. Res. 23, 2123. doi:10.1029/WR023i011p02123

Li, J., Heap, A.D., 2011. A review of comparative studies of spatial interpolation methods in environmental sciences: Performance and impact factors. Ecol. Inform. 6, 228–241. doi:10.1016/j.ecoinf.2010.12.003

Marcotte, D., 1996. Fast variogram computation with FFT. Comput. Geosci. 22, 1175–1180. doi:10.1016/S0098-3004(96)00026-X

Marshall, J.S., Gunn, K.L.S., 1952. Measurement of Snow Parameters by Radar. J. Meteorol. doi:10.1175/1520-0469(1952)009<0322:MOSPBR>2.0.CO;2

Marshall, J.S., Langille, R.C., Palmer, W.M.K., 1947. Measurement of Rainfall By Radar. J. Meteorol. 4, 186–192. doi:10.1175/1520-0469(1947)004<0186:MORBR>2.0.CO;2

Matheron, G., 1963. Principles of Geostatistics. Econ. Geol. 58, 1246–1266.

Mazzetti, C., Todini, E., 2009. Combining Weather Radar and Raingauge Data for Hydrologic Applications, in: Flood Risk Management: Research and Practice. Taylor & Francis Group, London.

McKee, J.L., Binns, A.D., 2015. A review of gauge–radar merging methods for quantitative precipitation estimation in hydrology. Can. Water Resour. J. / Rev. Can. des ressources hydriques 1784, 1–18. doi:10.1080/07011784.2015.1064786

Meneghini, R., 1978. Rain-rate estimates for an attenuating radar. Radio Sci. 13, 459–470.

Molini, A., Lanza, L.G., La Barbera, P., 2005. The impact of tipping-bucket raingauge measurement errors on design rainfall for urban-scale applications. Hydrol. Process. 19, 1073–1088. doi:10.1002/hyp.5646

Moszkowicz, S., Ciach, G.J., Krajewski, W.F., 1994. Statistical Detection of Anomalous Propagation in Radar Reflectivity Patterns. J. Atmos. Ocean. Technol. 11, 1026–1034. doi:10.1175/1520-0426(1994)011<1026:SDOAPI>2.0.CO;2

Nanding, N., Rico-Ramirez, M.A., Han, D., 2015. Comparison of different radar-raingauge rainfall merging techniques. J. Hydroinformatics 17, 422–445. doi:10.2166/hydro.2015.001

Nešpor, V., Sevruk, B., 1999. Estimation of wind-induced error of rainfall gauge measurements using a numerical simulation. J. Atmos. Ocean. Technol. 16, 450–464. doi:10.1175/1520-0426(1999)016<0450:EOWIEO>2.0.CO;2

Overeem, A., Leijnse, H., Uijlenhoet, R., 2013. Country-wide rainfall maps from cellular communication networks. Proc. Natl. Acad. Sci. 110, 2741–2745. doi:10.1073/pnas.1217961110

Pamment, J.A., Conway, B.J., 1998. Objective identification of echoes due to anomalous propagation in weather radar data. J. Atmos. Ocean. Technol. 15, 98–113. doi:10.1175/1520-0426(1998)0152.0.CO;2

Pappenberger, F., Beven, K.J., 2006. Ignorance is bliss: Or seven reasons not to use uncertainty analysis. Water Resour. Res. 42, 1–8. doi:10.1029/2005WR004820

Patterson, H.D., Thompson, R., 1971. Recovery of inter-block information when block sizes are unequal. Biometrika 58, 545–554. doi:10.1093/biomet/58.3.545

Pebesma, E.J., 2004. Multivariable geostatistics in S: The gstat package. Comput. Geosci. 30, 683–691. doi:10.1016/j.cageo.2004.03.012

Pegram, G., Llort, X., Sempere-Torres, D., 2011. Radar rainfall: Separating signal and noise fields to generate meaningful ensembles. Atmos. Res. 100, 226–236. doi:10.1016/j.atmosres.2010.11.018

Peleg, N., Ben-Asher, M., Morin, E., 2013. Radar subpixel-scale rainfall variability and uncertainty: lessons learned from observations of a dense rain-gauge network. Hydrol. Earth Syst. Sci. 17, 2195–2208. doi:10.5194/hess-17-2195-2013

Qi, Y., Zhang, J., Zhang, P., Cao, Q., 2013. VPR correction of bright band effects in radar QPEs using polarimetric radar observations. J. Geophys. Res. Atmos. 118, 3627–3633. doi:10.1002/jgrd.503642013

Rico-Ramirez, M.A., 2012. Adaptive Attenuation Correction Techniques for C-Band Polarimetric Weather Radars. IEEE Trans. Geosci. Remote Sens. 50, 5061–5071.

Rico-Ramirez, M.A., Cluckie, I.D., 2008. Classification of ground clutter and anomalous propagation using dual-polarization weather radar. IEEE Trans. Geosci. Remote Sens. 46, 1892–1904.

Rico-Ramirez, M.A., Gonzalez-Ramirez, E., Cluckie, I., Han, D., 2009. Real-time monitoring of weather radar antenna pointing using digital terrain elevation and a Bayes clutter classifier. Meteorol. Appl. 16, 227–236. doi:10.1002/met

Rico-Ramirez, M. a., Cluckie, I.D., 2007. Bright-band detection from radar vertical reflectivity profiles. Int. J. Remote Sens. 28, 4013–4025. doi:10.1080/01431160601047797

Rico-Ramirez, M. a., Cluckie, I.D., Han, D., 2005. Correction of the bright band using dual-polarisation radar. Atmos. Sci. Lett. 6, 40–46. doi:10.1002/asl.89

Rico-Ramirez, M. a., Liguori, S., Schellart, a. N. a., 2015. Quantifying radar-rainfall uncertainties in urban drainage flow modelling. J. Hydrol. 528, 17–28. doi:10.1016/j.jhydrol.2015.05.057

Ryzhkov, A. V., 2007. The impact of beam broadening on the quality of radar polarimetric data. J. Atmos. Ocean. Technol. 24, 729–744. doi:10.1175/JTECH2003.1

Sauvageot, H., 1992. Radar Meteorology. Artech House Inc, Norwood.

Sawicka, K., Heuvelink, G.B.M., 2016a. Software tools for quantifying uncertainty across different scales.

Sawicka, K., Heuvelink, G.B.M., 2016b. "spup" – an R package for uncertainty propagation in spatial environmental modelling, in: 12th International Symposium on Spatial Accuracy Assessment in Natural Resources and Environmental Sciences, Accuracy 2016. Montpellier, pp. 275–282.

Scheidegger, A., Rieckermann, J., 2014. Bayesian assimilation of rainfall sensors with fundamentally different integration characteristics, in: WRaH Proceedings. Washington.

Schilling, W., 1991. Rainfall data for urban hydrology: what do we need? Atmos. Res. 27, 5–21.

Schröter, K., Llort, X., Velasco-Forero, C., Ostrowski, M., Sempere-Torres, D., 2011. Implications of radar rainfall estimates uncertainty on distributed hydrological model predictions. Atmos. Res. 100, 237–245. doi:10.1016/j.atmosres.2010.08.014

Seed, A.W., Nicol, J.C., Austin, G.L., Stow, C.D., Bradley, S.G., 2007. The impact of radar and raingauge sampling errors when calibrating a weather radar. Meteorol. Appl. 3, 43–52. doi:10.1002/met.5060030105

Sevruk, B., 1996. Adjustment of tipping-bucket precipitation gauge measurements. Atmos. Res. 42, 237–246. doi:10.1016/0169-8095(95)00066-6

Sideris, I. V., Gabella, M., Erdin, R., Germann, U., 2014. Real-time radar-rain-gauge merging using spatio-temporal co-kriging with external drift in the alpine terrain of Switzerland. Q. J. R. Meteorol. Soc. 140, 1097–1111. doi:10.1002/qj.2188

Sinclair, S., Pegram, G., 2005. Combining radar and rain gauge rainfall estimates using conditional merging. Atmos. Sci. Lett. 6, 19–22. doi:10.1002/asl.85

Smith, C.J., 1986. The Reduction of Errors Caused by Bright Bands in Quantitative Rainfall Measurements Made Using Radar. J. Atmos. Ocean. Technol. 3, 129–141. doi:10.1175/1520-0426(1986)003<0129:TROECB>2.0.CO;2

Smith, P.L., 1984. Equivalent Radar Reflectivity Factors for Snow and Ice Particles. J. Clim. Appl. Meteorol. doi:10.1175/1520-0450(1984)023<1258:ERRFFS>2.0.CO;2

Snepvangers, J.J.J.C., Heuvelink, G.B.M., Huisman, J.A., 2003. Soil water content interpolation using spatio-temporal kriging with external drift. Geoderma 112, 253–271. doi:10.1016/S0016-7061(02)00310-5

Spadavecchia, L., Williams, M., 2009. Can spatio-temporal geostatistical methods improve high resolution regionalisation of meteorological variables? Agric. For. Meteorol. 149, 1105–1117. doi:10.1016/j.agrformet.2009.01.008

Stein, M.L., 1999. Interpolation of Spatial Data, Springer s. ed. Springer-Verlag, New York.

Steiner, M., Smith, J. a., 2002. Use of three-dimensional reflectivity structure for automated detection and removal of nonprecipitating echoes in radar data. J. Atmos. Ocean. Technol. 19, 673–686. doi:10.1175/1520-0426(2002)019<0673:UOTDRS>2.0.CO;2

Steiner, M., Smith, J. a., Burges, S.J., Alonso, C. V., Darden, R.W., 1999. Effect of bias adjustment and rain gauge data quality control on radar rainfall estimation. Water Resour. Res. 35, 2487. doi:10.1029/1999WR900142

Todini, E., 2001. A Bayesian technique for conditioning radar precipitation estimates to rain-gauge measurements. Hydrol. Earth Syst. Sci. 5, 187–199. doi:10.5194/hess-5-187-2001

Uijlenhoet, R., Berne, A., 2008. Stochastic simulation experiment to assess radar rainfall retrieval uncertainties associated with attenuation and its correction. Hydrol. Earth Syst. Sci. 12, 587–601. doi:10.5194/hess-12-587-2008

Upton, G.J.G., Rahimi, A.R., 2003. On-line detection of errors in tipping-bucket raingauges. J. Hydrol. 278, 197–212. doi:10.1016/S0022-1694(03)00142-2

Velasco-Forero, C. a., Sempere-Torres, D., Cassiraga, E.F., Jaime Gómez-Hernández, J., 2009. A non-parametric automatic blending methodology to estimate rainfall fields from rain gauge and radar data. Adv. Water Resour. 32, 986–1002. doi:10.1016/j.advwatres.2008.10.004

Velasco-Forero, C., Sempere-Torres, D., Sánchez-Diezma, R., Cassiraga, E., Gómez-Hernández, J., 2004. A non-parametric methodology to merge raingauges and radar by kriging: to errors in radar measuresensitivityments. ERAD 2004 Third Eur. Conf. Radar Meteorol. Hydrol. 21–24.

Vignal, B., Andrieu, H., Creutin, J.D., 1999. Identification of Vertical Profiles of Reflectivity from Volume Scan Radar Data. J. Appl. Meteorol. 38, 1214–1228. doi:10.1175/1520-0450(1999)038<1214:IOVPOR>2.0.CO;2

Villarini, G., Krajewski, W.F., 2010. Review of the different sources of uncertainty in single polarization radar-based estimates of rainfall. Surv. Geophys. 31, 107–129. doi:10.1007/s10712-009-9079-x

Villarini, G., Krajewski, W.F., 2009. Empirically based modelling of radar-rainfall uncertainties for a C-band radar at different time-scales. Q. J. R. Meteorol. Soc. 1438, 1424–1438. doi:10.1002/qj

Villarini, G., Krajewski, W.F., Ciach, G.J., Zimmerman, D.L., 2009. Product-error-driven generator of probable rainfall conditioned on WSR-88D precipitation estimates. Water Resour. Res. 45, 1–11. doi:10.1029/2008WR006946

Villarini, G., Mandapaka, P. V., Krajewski, W.F., Moore, R.J., 2008. Rainfall and sampling uncertainties: A rain gauge perspective. J. Geophys. Res. 113, D11102. doi:10.1029/2007JD009214

Villarini, G., Seo, B.C., Serinaldi, F., Krajewski, W.F., 2014. Spatial and temporal modeling of radar rainfall uncertainties. Atmos. Res. 135–136, 91–101. doi:10.1016/j.atmosres.2013.09.007

Wadoux, A.M..-C., Brus, D.J., Rico-Ramirez, M.A., Heuvelink, G.B.M., 2017. Sampling design optimisation for rainfall prediction using a non-stationary geostatistical model. Adv. Water Resour. 107, 126–138. doi:10.1016/j.advwatres.2017.06.005

Wauben, W.M.F., 2006. KNMI contribution to the WMO Laboratory Intercomparison of Rainfall Intensity Gauges.

Webster, R., Oliver, M.A., 2001. Geostatistics for Environmental Scientists (Statistics in Practice. Chichester.

Wessels, H.R.A., 2006. KNMI Radar Methods.

Wesson, S.M., Pegram, G.G.S., 2004. Radar rainfall image repair techniques 8, 220–234.

Westrick, K.J., Mass, C.F., Colle, B. a., 1999. The Limitations of the WSR-88D Radar Network for Quantitative Precipitation Measurement over the Coastal Western United States. Bull. Am. Meteorol. Soc. 80, 2289–2298. doi:10.1175/1520-0477(1999)080<2289:TLOTWR>2.0.CO;2

Wheater, H.S., Isham, V.S., Cox, D.R., Chandler, R.E., Kakou, A., Northrop, P.J., Oh, L., Onof, C., Rodriguez-Iturbe, I., 2000. Spatial-temporal rainfall fields: modelling and statistical aspects. Hydrol. Earth Syst. Sci. 4, 581–601. doi:10.5194/hess-4-581-2000

Whiton, R.C., Smith, P.L., Bigler, S.G., Wilk, K.E., Harbuck, A.C., 1998a. History of Operational Use of Weather Radar by U.S. Weather Services. Part I: The Pre-NEXRAD Era. Weather Forecast. 13, 219–242. doi:10.1175/1520-0434(1998)013<0244:HOOUOW>2.0.CO;2

Whiton, R.C., Smith, P.L., Bigler, S.G., Wilk, K.E., Harbuck, A.C., 1998b. History of Operational Use of Weather Radar by U.S. Weather Services. Part II: Development of Operational Doppler Weather Radars. Weather Forecast. 13, 244–252. doi:10.1175/1520-0434(1998)013<0244:HOOUOW>2.0.CO;2

Winterrath, T., Rosenow, W., Weigl, E., 2012. On the DWD quantitative precipitation analysis and nowcasting system for real-time application in German flood risk management, in: Weather Radar and Hydrology. Exeter, pp. 323–329.

Zhang, J., Qi, Y., 2010. A Real-Time Algorithm for the Correction of Brightband Effects in Radar-Derived QPE. J. Hydrometeorol. 11, 1157–1171. doi:10.1175/2010JHM1201.1

Zhang, X.F., Eijkeren, J.C.H.V.A.N., 1995. On the Weighted Least-Squares Method for Fitting a Semivariogram Model. Comput. Geosci. 21, 605–608.